

1 **A three year time-series of volatile organic iodocarbons in Bedford Basin, Nova Scotia :**
2 **a Northwestern Atlantic fjord.**

3
4 *Qiang Shi¹, Douglas Wallace¹*

5
6 ¹Department of Oceanography, Dalhousie University, Halifax, Canada
7 Email: qshi@dal.ca

8
9 **Abstract:**

10
11 We report weekly observations of volatile organic iodocarbons (CH₃I, CH₂ClI and CH₂I₂) over the
12 time-period May 2015 to December 2017 from 4 depths in Bedford Basin, a coastal fjord (70m
13 deep) on the Atlantic coast of Canada. The fjord is subject to winter-time mixing, seasonal
14 stratification and bloom dynamics, subsurface oxygen depletion, local input of freshwater and
15 occasional intrusions of higher density water from the adjacent continental shelf. Near-surface
16 concentrations showed strong seasonal and sub-seasonal variability which is compared with other
17 coastal time-series. The vertical variation of CH₂I₂ and CH₂ClI within the upper 10m is consistent
18 with rapid photolysis of CH₂I₂. Average annual sea-to-air fluxes (46.7 nmol m⁻² day⁻¹) of total
19 volatile organic iodine were similar to those observed in other coastal and shelf time-series and
20 polyiodinated compounds contributed 80% of the total flux. Fluxes were subject to strong
21 interannual variability (a factor of two) mainly due to wind-speed variability. Near-surface net
22 production of CH₃I averaged 1 pmol L⁻¹ day⁻¹ and was similar to rates in the English Channel but
23 an order of magnitude higher than in shallow waters of the Kiel Fjord, Germany, possibly due to
24 higher microbial degradation in the latter. The near-bottom (60 m) time-series showed evidence
25 for CH₃I production associated with organic matter degradation, and a possible “switch” from
26 production of CH₃I via an alkylation pathway to production of CH₂I₂ by a haloform-type reaction.
27 Near-bottom CH₃I production varied strongly between years but was generally ca. 20 times lower
28 than near-surface production.

1 **Keywords:** Iodocarbons, iodomethane, chloriodomethane, diiodomethane, air-sea flux, time-
2 series

3

4 1. Introduction

5 Volatile organic iodocarbons (VOIs) such as methyl iodide (CH_3I), chloriodomethane (CH_2ClI)
6 and diiodomethane (CH_2I_2) have a predominantly oceanic source and supply a significant amount
7 of iodine to the atmosphere (see review by Saiz-Lopez and Von Glasow, 2012). These gases, also
8 referred to as VSLS (very short-lived source gases) due to their reactivity and short atmospheric
9 lifetimes, have been implicated in supporting catalytic ozone destruction in the troposphere (Davis
10 et al., 1996; McFiggans et al., 2000) and, potentially in the lower stratosphere (Solomon et al.,
11 1994) as well as aerosol formation in the marine boundary layer (McFiggans et al., 2000, 2004;
12 O'Dowd et al., 2002). Recent modelling of atmospheric reactive iodine ($\text{IO}_x = \text{IO} + \text{I}$) as well as
13 experimental studies (Carpenter et al., 2013; Jones et al., 2010; Mahajan et al., 2010) suggest that
14 the supply of volatile organoiodine represents <50% of the total sea-to-air delivery of reactive
15 iodine, with most being supplied in the form of HOI and I_2 . Nevertheless, the potential for localized
16 higher emissions coupled with their relatively long lifetimes (compared to I_2 and HOI) allows the
17 organic compounds to be a significant source of iodine to the free troposphere and even, potentially,
18 to the lower stratosphere in certain regions (Tegtmeier et al., 2013). Further, Mahajan et. al (2012)
19 noted a strong correlation of IO_x and CH_3I suggesting that the sources of CH_3I and the shorter-
20 lived precursors of IO_x are closely related or depend on similar variables.

21 CH_3I is the most abundant VOI species in the atmosphere (Yokouchi et al., 2011) because of its
22 longer lifetime (days) compared to CH_2ClI (hours) and CH_2I_2 (minutes) (Moessinger et al., 1998;
23 Rattigan et al., 1997). However, the total supply of organically-bound iodine to the atmosphere is

1 several times larger than the CH_3I supply alone (Carpenter et al., 2014) with the bulk of the
2 remainder transported in the form of CH_2I_2 and CH_2ClI (additional iodocarbons such as $\text{CH}_3\text{CH}_2\text{I}$,
3 CH_2BrI and CHI_3 are generally present in much lower concentration). Despite considerable
4 attention on the oceanic distribution and sea-to-air flux of these compounds, in particular CH_3I
5 (Ziska et al., 2013), it is not yet possible to apportion oceanic production of these compounds,
6 unequivocally, to specific mechanisms. Even for CH_3I , controversy remains, for example, as to
7 the relative importance of direct “biological” or “photochemical” production pathways with
8 experimental evidence reported for both, and correlation analysis generally being inconclusive, in
9 part because of the “snapshot” nature of most studies (Stemmler et al., 2014). Comparisons of
10 models to observed distributions have also proven ambiguous, with localized studies suggesting
11 predominance of a biological production pathway (Stemmler et al., 2013) but a global analysis
12 emphasising photochemical production as the dominant mechanism. This diversity of views has
13 been maintained through a variety of experimental studies (Amachi et al., 2001; Brownell et al.,
14 2010; Hughes et al., 2011; Manley and delaCuesta, 1997; Moore and Tokarczyk, 1993; Moore and
15 Zafiriou, 1994; Richter and Wallace, 2004; Shi et al., 2014a; Smythe-Wright et al., 2006).

16 For compounds other than CH_3I , similar uncertainty exists concerning production pathways, but
17 with fewer underlying studies. Laboratory experiments have shown that the presence of dissolved
18 iodide and dissolved organic matter can lead to production of these compounds in the dark
19 (Martino et al., 2009). Fuse et al. (2003) and Martino et al. (2005) observed that CH_2ClI could be
20 produced by photolysis of CH_2I_2 in artificial and natural seawater. However detailed mechanisms
21 and, especially, their relative importance in the field remain unclear.

22 Time-series observation can reveal processes and controlling factors underlying production and
23 loss of iodocarbons in the ocean and provide data for testing hypotheses and/or models. However,

1 only a very few long-term, time series observations of iodocarbons have been reported to date, all
2 from coastal water. Klick (1992) reported 13 months of weekly measurements of CH_2I_2 and
3 CH_2ClI from very shallow (3.5m) water in the Kattegat at the Swedish coast. Orlikowska and
4 Schulz-Bull (2009) reported a year of weekly data for CH_2ClI , CH_2I_2 , CH_3I and $\text{C}_2\text{H}_5\text{I}$ from a
5 nearshore (3m depth) site in the Baltic Sea. Archer et al. (2007) reported a seasonal study of
6 CH_2ClI , CH_2I_2 , CH_3I , $\text{C}_2\text{H}_5\text{I}$, and CH_2BrI measured weekly at 4 depths (0-50m) in the western
7 English Channel from July 2002 to April 2004. Shi et al. (2014b) reported on the seasonal cycle
8 of CH_3I from surface waters of the Kiel Fjord: a shallow (14 m), brackish water body in northern
9 Germany, which was sampled weekly for 2 years. Shimizu et. al (2017) presented a time-series of
10 vertical profiles (0-90m) of CH_2I_2 , CH_2ClI , CH_3I , and $\text{C}_2\text{H}_5\text{I}$ from the centre of Funaka Bay, Japan,
11 which were measured every 2-4 weeks from March 2012 to December 2014.

12 Here, we report weekly observations of CH_3I , CH_2ClI and CH_2I_2 made over the time-period May
13 2015 to December 2017 at 4 depths (0-60m) in Bedford Basin: a coastal fjord on the east coast of
14 Canada. We report seasonal to interannual variability of the observed concentrations at different
15 depths in the water column and compare our results with the other time-series. We report daily
16 average fluxes to the atmosphere and use a simple, time-varying mass-balance model for near-
17 surface waters to estimate production rates and their variability. We discuss the observed
18 variability of both concentrations and production rates in the light of earlier studies, potentially
19 correlated variables and suggested production pathways.

20

21 2. Methods

22 Time-series measurements of VOIs were carried out in the Bedford Basin (44.69 °N, -63.63 °E)
23 near Halifax, Canada. Bedford Basin is an 8 km long, 17 km² fjord with a maximum depth of 71m

1 and a total volume of 500 km³. The Bedford Basin is connected with continental shelf waters of
2 the Atlantic Ocean through “the Narrows” (a ca. 300 m wide and 20 m deep passage (Fig. 1)). The
3 Basin receives freshwater primarily from the Sackville River at its northwestern end, with a total
4 average freshwater input of 5.41 m³ s⁻¹ (Buckley and Winters, 1992). The average near surface
5 salinity within the Basin is 29 which can be compared with salinities of >30 over the adjacent
6 Scotian Shelf. There are only relatively small horizontal gradients of near-surface salinity within
7 the Bedford Basin itself (typically < 2 difference from close to the Sackville River mouth to the
8 Narrows).

9 Time series observations of physical, chemical and biological parameters have been recorded since
10 1992 (Li, 1998). Our halocarbon samples were collected weekly, in the center of the Bedford Basin,
11 at its deepest point (Fig. 1), between May 2015 and January 2018. Samples were collected with
12 10-L Niskin bottles attached to a rosette sampler at 1, 5, 10 and 60 m (10 m samples were collected
13 biweekly from May to September 2015). The upper three water samples covered the majority of
14 the euphotic zone. The 60m water sample was from typically stagnant, near-bottom water which
15 is renewed by vertical mixing events in late winter, and by occasional intrusions of higher-salinity
16 continental shelf water in both summer and winter. Chlorophyll *a* (Chl*a*), dissolved oxygen, and
17 nutrients were measured weekly at the 4 depths as part of the Bedford Basin Monitoring Program
18 (Details can be found in website: [http://www.bio-iob.gc.ca/science/monitoring-monitorage/bbmp-](http://www.bio-iob.gc.ca/science/monitoring-monitorage/bbmp-pobb/bbmp-pobb-en.php)
19 [pobb/bbmp-pobb-en.php](http://www.bio-iob.gc.ca/science/monitoring-monitorage/bbmp-pobb/bbmp-pobb-en.php)). In addition to the Niskin bottle sampling, vertically continuous
20 measurements of temperature, salinity, dissolved oxygen and Chl *a* properties were measured with
21 a CTD mounted on the rosette. Additional information concerning the measurements of supporting
22 physical and biological parameters can be found in the paper by Burt et al. (2013).

1 The concentrations of iodomethane (CH_3I), chloriodomethane (CH_2ClI) and diiodomethane
2 (CH_2I_2) reported here, as well as of a number of other halocarbons (data not shown), were
3 measured using purge & trap gas chromatography with detection by both mass spectrometry (MS)
4 and electron capture (ECD). All measurements were made using an Agilent Technologies gas
5 chromatograph (GC 7890B), equipped with a capillary column (RTX-VGC; 60 m; 1.4 μm coating,
6 column diameter: 0.25 mm; helium carrier gas 0.5 ml min^{-1}), together with an automated purge
7 and trap system equipped with an autosampler (VSP4000 of IMT, Vohenstrauß, Germany). The
8 GC column was temperature programmed as follows: initial temperature 50 °C for 6 minutes, then
9 ramped to 150 °C at 6 °C min^{-1} ; ramped to 200 °C at 10 °C min^{-1} . Water samples (10 ml) were
10 stored in 20 ml vials equipped with an ultra-low-bleed septum, prior to purging with helium (20
11 ml min^{-1} for 18 mins). Every sample was analysed in triplicate. The standard deviation of triplicate
12 measurements (integrated peak area) was <10 % for CH_3I , <15 % for CH_2ClI and <20 % for CH_2I_2 .

13 Calibration of the GC system for CH_3I , CH_2ClI and CH_2I_2 was performed using permeation tubes
14 (VICI, Houston, TX, USA) which were maintained at a constant temperature of 23 °C and weighed
15 every 2 weeks. Dilutions of the permeation tube effluent were made in ultra-high-purity N_2
16 (>99.995 %) with flow rates of 50 to 700 ml min^{-1} , and samples were injected into the purge and
17 trap system (VSP) through a 140 μl loop. Standard deviation of the peak area during these
18 calibration runs was <5 % for CH_3I and CH_2ClI and <15 % for CH_2I_2 . Overall the calibration
19 response varied by less than 15 % over the entire sampling period.

20 Throughout the paper, seasons are defined as follows: summer is June through August; fall is
21 September through November; winter is December through February and spring is March to May.
22
23

1 3. Results and discussion

2 3.1 Environmental Variables from the Bedford Basin

3 The vertical profiles of temperature, salinity, dissolved oxygen and fluorescence (Fig. 2) are well-
4 mixed from top to bottom in late winter (Feb-Mar) as a result of wind-mixing and convection (Li,
5 2001). Temperature is marked by strong seasonality to depths of <30 m. Near-surface temperatures
6 start to rise above winter values of 4 °C, and stratified conditions develop, around early April with
7 temperatures reaching ca. 21 °C by the end of August (Fig. 2a).

8 Salinity ranges from 23 to 31 through the entire water column, with the lowest salinities occurring
9 very close to the surface (Fig. 2b and Fig. 3c). The near-surface stratification varied both seasonally
10 and between years, primarily in association with variability of precipitation and the discharge of
11 the Sackville River (source: Environment and Climate Change Canada;
12 http://climate.weather.gc.ca/historical_data/search_historic_data_e.html). For example, the
13 salinity at 1m was more than 1psu lower than at 5m during much of the summer of 2015 (June to
14 September) and summer 2017 (June to August). In summer 2016, however, the salinity at 1m was
15 close to that at 5m (difference < 0.3) (Fig. 3c). Occasional intrusions of more dense water from the
16 Scotian Shelf, results in increased salinity, especially of bottom waters. The intrusions are irregular
17 and tend to occur a few times per year, for instance in May 2016 at which time the salinity of
18 bottom water increased from 30.8 to 31.0 (Fig. 2b), and in early July 2017 when the salinity of
19 mid-depth water increased from 30.5 to 31 (see marked circle in Fig. 2b).

20 The dissolved oxygen time-series (Fig. 2c) shows the effect of temperature-dependent solubility
21 variations in surface waters as well as intrusions and late-winter vertical mixing in deeper water.
22 In surface water the highest O₂ concentrations occurred between March and April every year in
23 association with lowest seawater temperature. The vertical gradient of O₂ concentration was,

1 generally, smallest towards the end of April as a result of vertical mixing. Sub-surface O₂
2 concentrations (>30 m) generally decreased in summer due to respiration, with occasional
3 interruptions of this O₂ decline (e.g. November 2016) as a consequence of shelf-water intrusions
4 which brought sudden increases in O₂ levels.

5 Fig. 3 depicts time-depth plots of the variation of chlorophyll *a*, total dissolved inorganic nitrogen
6 (DIN = [NH₄⁺] + [NO₂⁻] + [NO₃⁻]), salinity, precipitation, windspeed and solar irradiance in
7 Bedford Basin over the period of the VOIs sampling. The seasonal variations of chlorophyll *a*
8 concentration in surface water (Fig. 3a) show that two blooms (spring and autumn) occur in surface
9 water. For example, in 2016, chlorophyll *a* increased rapidly from March to April (from 5 to 26
10 μg L⁻¹), and from September to October (from 10 to 28 μg L⁻¹). The vertical variation of
11 chlorophyll *a* (as determined from fluorescence measured on the CTD, see Fig. 2d) reached 12 μg
12 L⁻¹ during the bloom period. Sub-surface (20- 40 m) fluorescence-derived chlorophyll *a* dropped
13 down to 4 μg L⁻¹. In the near-bottom water chlorophyll *a* ranged between 0 and 2 μg L⁻¹ during
14 the whole year and varied only slightly.

15 The seasonal variation of dissolved inorganic nitrogen(DIN) in surface water is plotted in Fig. 3b.
16 In winter, when chlorophyll *a* levels are very low due to light limitation, DIN concentrations reach
17 ca. 12 μmol L⁻¹ but are drawn down to low levels (< 1 μmol L⁻¹) after the spring bloom.
18 Summertime chlorophyll *a* levels are moderate but variable (ca. 3 to 10 μg L⁻¹), likely reflecting
19 continuing nutrient input (e.g. from runoff and/or sewage treatment plants). The average
20 precipitation in Bedford Basin was 27.6 mm week⁻¹ in summer 2015 and was 16 mm week⁻¹ in
21 summer 2016 (Fig. 3d). Typically, strongest irradiance (data was downloaded from the CERES
22 FLASHFLUX system: <https://power.larc.nasa.gov/cgi-bin/hirestimeser.cgi>) occurs in June and
23 July (see Fig. 3f), and highest water temperatures are observed in August.

1 3.2 Variations of Iodocarbons Concentrations in Bedford Basin

2 Iodocarbon concentrations in surface water (1, 5 and 10 m) showed strong seasonality, with lowest
3 concentrations from December through May (1.2 pmol L⁻¹ for CH₃I; 1.3 pmol L⁻¹ for CH₂ClI and
4 0.3 pmol L⁻¹ for CH₂I₂). Concentrations start to increase in late May/ June, reaching levels as high
5 as 45 pmol L⁻¹ for CH₃I; 160 pmol L⁻¹ for CH₂ClI and ca. 80 pmol L⁻¹ for CH₂I₂ (with a single
6 peak of 500.5 pmol L⁻¹; Fig. 4). Near-surface, summertime concentrations of all three compounds
7 were characterized by a broad seasonal peak of 6-7 months duration (or shorter for CH₂I₂), on top
8 of which were superimposed ca. 3-4 peaks of ca. 1 month duration. The number, amplitude and
9 timing of these peaks varied amongst the three compounds with CH₃I, notably, showing only one
10 large peak in 2016 and four during the other two years of the time-series (Fig. 4a).

11 Concentrations at 60 m were almost always lower, and much less variable, ranging over the year
12 from 1 to 9 pmol L⁻¹ for CH₃I (except the Fall/Winter 2015-2016, see below), 1 to 6 pmol L⁻¹ for
13 CH₂ClI and 0.4 to 18 pmol L⁻¹ for CH₂I₂ (Fig. 4d) respectively. Hence, the bottom water (60 m)
14 concentrations of CH₂I₂ and CH₂ClI were always much lower than in near-surface waters
15 throughout the summers. The surface to deep concentration difference was smallest for CH₃I and
16 showed interannual variability. Notably bottom water concentrations reached 26 pmol L⁻¹ and were
17 even higher than in contemporary surface waters from September 2015 to March 2016 (Fig. 4d).
18 Missing from the bottom water time-series, were the ca. 1 month duration variations seen in
19 summertime surface water.

20 Inter-relations between the iodocarbons in surface seawater were examined with linear regression
21 of both weekly and monthly-averaged concentrations. The resulting correlations are shown in
22 Table 1. Using weekly data, significant correlations (i.e. p<0.05) were found between [CH₃I] and
23 [CH₂ClI] at 1, 5 and 10 m depths with the strongest correlation (0.7) at 10m. The only other

1 significant correlation was between CH₂I₂ and CH₂ClI at 5 m. Use of monthly averaged values
 2 gave stronger correlations. Once again, the significant correlations were between CH₃I and CH₂ClI
 3 (at 1, 5 and 10m depth) as well as between CH₂ClI and CH₂I₂ at 5 and 10m depth. Table 2 also
 4 presents the correlations of iodocarbon concentrations with potentially related variables (discussed
 5 in section 4.3).

6 Generally, the concentration of CH₂I₂ was higher than that of CH₂ClI. The average ratio of
 7 CH₂I₂/CH₂ClI within the top 10m of the water column over the summer months was 1.4. However,
 8 this ratio was significantly lower at 1m depth (average of 0.6) and increased with depth (1.5 at 5
 9 m and 2.2 at 10 m, reaching values as high as 2.7 at 60 m).

10

11 3.3 Sea-to-Air Flux

12 Using the concentrations of CH₃I, CH₂ClI and CH₂I₂ at 1m depth (Fig. 4) we estimated the sea-to-
 13 air flux of VOIs (F) using the following equation and the parameterization of Nightingale et al.,
 14 2000) for the water-side transfer velocity:

$$15 \quad Flux = K(C_{aqu} - C_{air} \times H) \quad (1)$$

$$16 \quad K_w = \left(\frac{Sc}{660}\right)^{-0.5} (0.222 \cdot u_{10}^2 + 0.333 \cdot u_{10}) \quad (2)$$

17 where u_{10} is windspeed at 10 m height, Sc is the temperature-dependent Schmidt number, as
 18 estimated by Groszko (1999) and Henry's Law constants (H) were from Moore et al. (1995). The
 19 air-side resistance has been shown by Archer et al. (2007) to be significant for soluble gases such
 20 as CH₂ClI and CH₂I₂. Hence K in equation 1 is calculated as follows (Liss and Slater, 1974):

$$21 \quad \frac{1}{K} = \frac{1}{K_w} + \frac{1}{HK_a} \quad (3)$$

22 where the air-side transfer velocity was calculated according to Duce et al. (1991).

$$23 \quad K_a = u_{10}/(770 + 45(MW)^{1/3}) \quad (4)$$

1 with MW being the molecular weight of the gas of interest.

2 Daily averaged wind speed was measured at the nearby Halifax Dockyard (Fig. 1) (source:
3 Environment and Climate Change Canada; http://climate.weather.gc.ca/index_e.html). Seawater
4 temperature and surface iodocarbon concentrations were interpolated linearly between the weekly
5 measurements in order to coincide with the wind speed data and generate daily flux estimates.

6 Following Archer et al. (2007) and Shimizu et al. (2017), we applied an atmospheric concentration
7 of zero for calculating the flux of all three compounds. Rasmussen et al. (1982) reported an average
8 atmospheric mixing ratio of CH₃I of ca. 1 pptv for Cape Meares (45 °N) and Yokouchi et al. (2008)
9 presented a mean concentration of 0.98 pptv for Cape Ochiishi (43.2 °N), with both sites sharing
10 a similar latitude to our sampling location (44.69 °N). If a mixing ratio of 1pptv had been used for
11 our calculations, the total annual flux of CH₃I would be reduced by only 5 %. Atmospheric mixing
12 ratios of CH₂ClI and CH₂I₂ are generally lower (reviewed by Carpenter, 2003) so that any
13 overestimation of the fluxes of these compounds due to this assumption will certainly be negligible
14 (Archer et al., 2007).

15 Fig. 5 presents the weekly averaged combined flux of organically-bound iodine, $F_{I_{org}}$, as stacked
16 bar charts, where $F_{I_{org}} = (F_{CH_3I} + F_{CH_2ClI} + 2 * F_{CH_2I_2})$. The calculated emissions of individual
17 compounds ranged from 0.9 to 39.2 nmol m⁻² d⁻¹ for CH₃I (annual average of 8.4 nmol m⁻² d⁻¹),
18 0.9 to 78.0 nmol m⁻² d⁻¹ for CH₂ClI (annual average of 17.4 nmol m⁻² d⁻¹) and 0.3 to 78.0 nmol m⁻²
19 d⁻¹ for CH₂I₂ (annual average of 10.3 nmol m⁻² d⁻¹). Seasonal and annual average fluxes of the
20 individual compounds and of I_{org} are presented in Table 3. Clearly the sea-to-air flux is highest in
21 summer and fall and is dominated by the flux of the dihalomethanes rather than CH₃I.

22

23

1 3.4 Net Production of CH₃I

2 We used a mass balance approach to estimate the production rate of CH₃I within the uppermost
3 10m of the water column, based on the concentration time-series (see also Shi et al., 2014b). Using
4 the annual cycle of average near-surface CH₃I concentrations (Fig. 4a), we examined the mass
5 balance of CH₃I for this fixed depth interval according to:

$$6 \quad \Delta C = P_{net} - L_{sea-to-air} - L_{SN2} - L_{mix} \quad (5)$$

7 where ΔC is the daily change of the average CH₃I concentration in the near-surface seawater (0-10
8 m); P_{net} represents the net of gross production minus any additional, uncharacterized losses such
9 as microbial degradation; $L_{sea-to-air}$ is the sea-to-air flux (section 3.3) and L_{SN2} is the ‘chemical’ loss
10 due to nucleophilic substitution of Cl⁻ for I⁻ which was calculated based on reaction kinetics (Elliott
11 and Rowland, 1993; Jones and Carpenter, 2007) using the corresponding temperature, salinity and
12 mean concentration of CH₃I. L_{SN2} averaged 0.1 pmol L⁻¹ day⁻¹. L_{mix} is the loss due to downward
13 mixing and has been shown in several studies to be negligible compared with other loss terms e.g.
14 (Richter and Wallace, 2004). The latter assumption will not always be valid in winter and,
15 especially, when mixed layers deepen to >10m. However most production of iodocarbons occurs
16 during summer and fall when there is strong stratification within the upper 10m (see Fig. 3c), and
17 we excluded from our mass balance calculations the limited periods of time when density was
18 uniform in this depth interval.

19 The net production rate of CH₃I over the 3-year time-series is shown in Fig. 6. The annual average
20 production rate of CH₃I was 1.0 pmol L⁻¹ day⁻¹ (ranging from -1.6 to 8.5 pmol L⁻¹ day⁻¹). A
21 significant peak of P_{net} occurred from August to September in every year. The net production rate
22 of CH₃I in summer and fall averaged 1.6 pmol L⁻¹ day⁻¹ and was 5 times larger than wintertime
23 rates (ca. 0.3 pmol L⁻¹ day⁻¹). Net production rates for CH₂ICl and CH₂I₂ were also calculated

1 (results not shown), with typical summertime values being 3.2 and 1.3 pmol L⁻¹ day⁻¹, respectively.
2 Photolytic loss can be very significant for these compounds and has not been estimated, so these
3 P_{net} values represent the net of gross production minus uncharacterized losses including photolysis
4 as well as microbial degradation.

5

6 4. Discussion

7 In the following we discuss the Bedford Basin data in comparison with other studies that have
8 reported concentrations of multiple iodocarbons and especially those that have reported time-series
9 covering an annual cycle (see citations in the introduction). All of these time-series are from mid-
10 latitude (40-60°N) nearshore or continental shelf environments subject to strong seasonal
11 variations of light, temperature and biological productivity. There are no reported time-series of
12 seawater concentrations from low latitudes.

13

14 4.1 Potential influence of nearshore and /or macroalgal sources

15 The potential of nearshore macroalgae to cause elevated coastal iodocarbon concentrations has
16 been mentioned in a number of studies (Giese et al., 1999; Manley and delaCuesta, 1997; Schall
17 et al., 1994). We investigated this in July 2017, by sampling at 5 nearshore sites around Bedford
18 Basin (Fig. 1) and comparing nearshore concentrations with values measured at the regular
19 sampling site in the center of the Basin (Table 4). The nearshore results were consistently within
20 one standard deviation of mean concentrations of VOIs measured at the center of Bedford Basin
21 during July, indicating no significant difference. Klick (1992) also compared measurements on
22 samples collected directly over a rich bed of macroalgae with samples collected further away from
23 direct contact with macroalgae: whereas they observed significantly higher concentrations of

1 bromocarbons in proximity to the macroalgae, there was no difference observed for CH_2I_2 and
2 CH_2ClI . Shimizu et al. (2017) sampled a number of nearshore regions around Funka Bay, including
3 rocky shores with extensive macroalgae, and also found concentrations to be similar at both
4 nearshore and central Bay locations. We therefore conclude that any direct impact of macroalgae
5 on measured organoiodine levels is small, even in coastal regions, which lends strong support to
6 the conclusion by Saiz-Lopez and Von Glasow (2012) that macroalgae are only a minor global
7 source of these compounds to the atmosphere.

8

9 4.2 Concentrations and relative abundance of iodocarbon compounds

10 The average concentration of total volatile organic iodine I_{org} (where $I_{\text{org}} = [\text{CH}_3\text{I}] + [\text{CH}_2\text{ClI}] +$
11 $2[\text{CH}_2\text{I}_2]$) and the relative contributions of the different compounds to I_{org} from this and other
12 studies is shown in F. The combined concentrations of the three iodocarbons are highest but also
13 show highest variability ($[I_{\text{org}}] = 25$ to 281 pmol L^{-1}) in summertime coastal waters (loosely defined
14 here as within a few kms of land). Continental shelf waters have lower concentrations of I_{org}
15 averaging 32 pmol L^{-1} , with open ocean waters having comparable or lower concentrations
16 (average $I_{\text{org}} = 17 \text{ pmol L}^{-1}$). Despite the differences in I_{org} concentration ranges evident for
17 different regions in Fig. 7, a 1-way ANOVA showed no significant differences between the means
18 for the three regions. However after pooling of shelf and open ocean results to make only two
19 populations, a t-test did reveal a significant difference with coastal waters for at the 95%
20 confidence level.

21 The distribution of I_{org} is contrary to the global distribution of CH_3I reported by Ziska et al. (2013)
22 who noted a tendency for the open ocean to have higher concentrations than coastal waters (their
23 definition of “coastal” was within 1 degree latitude or longitude of land and therefore much broader

1 than ours). As noted by Ziska et al. (2013), this may reflect higher CH₃I concentrations in tropical
2 and sub-tropical open ocean waters, as their general pattern was reversed in the Northern
3 Hemisphere. The coastal waters depicted in Fig. 7 are largely from mid-latitudes of the Northern
4 Hemisphere.

5 The relative contribution of the dihalomethanes to I_{org} also appears to vary between regions, with
6 the ratio of dihalomethane-I to I_{org}, ($[\text{CH}_2\text{CII}] + 2 * [\text{CH}_2\text{I}_2] / [\text{I}_{\text{org}}]$), averaging 0.71, 0.69 and 0.55 in
7 coastal, shelf and open ocean waters, respectively. While an elevated contribution of
8 dihalomethanes in coastal waters is consistent with the report by Jones et al. (2010), regional
9 differences apparent in Fig. 7 are not significant at the 95% confidence level when tested with a 1-
10 way ANOVA.

11 Klick (1992), Jones et al. (2010) and Shimizu et al. (2017) reported concentrations of volatile
12 organic iodine in summertime coastal waters that are comparable to, or higher than those observed
13 in Bedford Basin (i.e. average I_{org} concentrations >100 pmol L⁻¹). Our results from Bedford Basin
14 correspond closely with concentrations and relative contributions reported by Shimizu et al. (2017)
15 for coastal water in Funka Bay, Japan (Fig. 7). In these coastal surface waters, the CH₂I₂
16 concentration and contribution was highest on average, followed by CH₂CII and the lowest was
17 CH₃I. In open ocean waters, the relative contribution of [CH₃I] to I_{org} appears higher, reaching
18 over 50% in some cases (see Fig. 7), with the contribution of CH₂I₂ generally being lower in the
19 open ocean than in coastal waters. However, once again, these apparent regional differences are
20 not significant at the 95% confidence level.

21 In laboratory studies, Fuse et al. (2003) demonstrated that relatively large amounts of CH₂I₂ and
22 I₂ together with smaller but still significant amounts of CH₂CII and CHI₃ can be produced,
23 presumably abiotically, in dark incubations of (filtered) spent culture media with suspended

1 bacterial cells and added $[I^-]$. The CH_2I_2/CH_2ClI production ratio was ~ 35 and no mono-iodinated
2 CH_3I was produced in these experiments. The implication was that dissolved organic compounds
3 within spent media were key to production of polyiodinated compounds. In the absence of spent
4 culture media, additions of oxaloacetic acid also resulted in formation of CH_2I_2 and CH_2ClI (with
5 a lower ratio of CH_2I_2/CH_2ClI of ~ 10) suggesting that organic acids may be a substrate for their
6 formation. The mechanistic role of the suspended bacterial cells was not clear, however they may
7 have supplied haloperoxidases required for oxidation of I^- (see also Hill and Manley, 2009).
8 Martino et. al (2009) demonstrated that, alternatively, oxidation of dissolved iodide to I_2 and HOI
9 by reaction with ozone (e.g. Garland et al., 1980) in filtered ($0.2 \mu m$) seawater containing natural
10 levels of dissolved organic matter also resulted in formation of polyiodinated compounds (CH_2I_2 ,
11 CH_2ClI and CHI_3) with CH_2I_2/CH_2ClI production ratios ranging from 2 to 4. They suggested that
12 the yield of various iodocarbons depends on “the abundance and perhaps on the nature of the
13 organic substrate” which “can vary widely both temporally and spatially”. We could not, however,
14 find any obvious relationship of near-surface iodocarbon concentrations with local measurements
15 of atmospheric ozone near Bedford Basin (results not shown).
16 We therefore suggest that the higher levels of CH_2I_2 observed in coastal waters, including Bedford
17 Basin, reflect a higher supply rate of HOI and/or I_2 and/or of the organic precursors suitable for
18 formation of polyiodinated compounds. Ultimately, reduction of seawater iodate to reduced forms,
19 such as iodide, likely supports the potential for organoiodine formation. Addition of iodide has
20 been identified, in short-term experiments, as a source for reactive iodine (iodine atoms) which
21 can stimulate photochemical formation of CH_3I (Moore and Zafiriou, 1994). However, Shi et. al
22 (2014b) found no positive correlation of $[I^-]$ with seasonal CH_3I production in a field study in Kiel
23 fjord, noting that background iodide levels may have been always sufficient to support production

1 of pM levels of CH₃I. Indeed, there is no *a priori* reason to expect a positive correlation of [I⁻] with
2 iodocarbon production if supply of more reactive iodine species (iodine atoms, HOI and/or I₂) is
3 the key, proximate control. The short-term formation rate of reactive species from a background
4 reservoir of I⁻, and hence production of iodocarbons, may depend more on availability of
5 haloperoxidases, various oxidants and/or temperature-dependent kinetics. The conversion of I⁻ to
6 these reactive species could even lead to inverse correlations between I⁻ and iodocarbons.
7 Relatively small quantities of CH₂ClI were produced in several of the experiments cited above,
8 yet observations in Bedford Basin show average CH₂I₂/CH₂ClI ratios of 1.4 in the top 10 m of the
9 water column. Production ratios in these experiments vary, as noted above, but laboratory studies
10 have also shown that photolysis of CH₂I₂ can be an important source of CH₂ClI in surface waters
11 with a yield of 25 % to 35 % (Jones and Carpenter, 2005; Martino et al., 2005). We observed
12 significant correlation between [CH₂I₂] and [CH₂ClI] at 5 and 10 m depth (but not at 1m)(Table
13 1), which is consistent with a fraction of the CH₂I₂ production being transformed photochemically
14 (The lack of correlation at 1m may be due to the very rapid photolysis). However the correlation
15 may also reflect the original production ratio of the individual compounds (which laboratory
16 experiments suggest may be substrate-dependent). In both cases however, DOM quality and
17 quantity (possibly associated with terrestrial supply) and/or elevated supply of I⁻ are likely to be
18 underlying reason(s) for the high concentrations of dihalomethanes observed in Bedford Basin and
19 other coastal waters.

20

21 4.3 Temporal variations of iodocarbons in near-surface water

22 The following discussion of temporal variability is separated into consideration of seasonal and
23 interannual variations.

1 4.3.1 Seasonal Variations

2 All of the reported iodocarbon time-series showed strong seasonality, with minimum, sometimes
3 undetectable concentrations in winter, and higher concentrations in summer. Near-surface (0-10
4 m) concentrations of all three iodocarbons in Bedford Basin, including CH₃I, remained low until
5 mid-May to mid-June, with their subsequent increase coincident with initial warming of near-
6 surface waters from wintertime minimum temperatures of ca. 1-2 °C (lag < 1 month; Fig. 8a).
7 Hence the initial appearance of all three iodocarbons occurred more than 3 months after the
8 seasonal increase in solar radiation, ca. 1-2 months after the Spring Bloom (Fig. 8d), after near-
9 surface nitrate had been drawn down to low levels (Fig. 8e) and almost coincident with the seasonal
10 temperature increase (Fig. 8a).

11 In the western English Channel (Archer et al., 2007), a gradual increase of CH₃I commenced in
12 February, coincident with the seasonal increase in solar radiation. Summertime values remained
13 high, with some higher-frequency variation, and then decreased in September/October. The
14 increase of CH₂ClI and CH₂I₂ started later, in April, more or less coincident with both the Spring
15 Bloom and initiation of near-surface warming from a wintertime minimum temperature of ca. 8
16 °C. Summertime values of CH₂ClI and CH₂I₂ showed periodic variations similar to those observed
17 in Bedford Basin (section 3.2).

18 The lower temporal resolution of the study in Funka Bay (Shimizu et al., 2017), with sampling
19 only every 1 or 2 months, precluded detailed examination of timing. A gradual increase in CH₃I
20 appeared to start in March, during or towards the end of the Spring Bloom when surface water
21 temperatures were still close to their wintertime minimum of -1 to 2.5 °C. The seasonal increase
22 of CH₂I₂ and CH₂ClI occurred later (May-June) at a time of rising water temperatures and low

1 nutrient levels with concentrations remaining elevated through the summer and decreasing to
2 wintertime levels in October.

3 The initial CH₃I increase at a shallow station in the Kiel Fjord (Shi et al., 2014b) occurred in March,
4 and was closely linked in time to seasonal increases of solar radiation, temperature (winter
5 minimum of 0 °C) as well as Chl *a* and the springtime drawdown of nitrate. Lagged correlation
6 analysis showed similarly strong correlations of CH₃I with both temperature and solar radiation,
7 with the annual cycle of CH₃I lagging temperature by ca. 1 month, however the very close
8 correspondence of multiple seasonal cycles led the authors to note that “the use of correlation
9 analysis to infer causality has likely reached its limit in this analysis”.

10 The observation of a rapid increase in the production rate of I⁻ within phytoplankton cultures
11 (diatoms and prymnesiophytes) when they enter stationary and, especially, senescent phases
12 (Bluhm et al., 2011) is potentially relevant to the observed seasonality of iodocarbon formation.

13 The reduction of iodate to iodide was suggested to be due to release of precursors, such as reduced
14 sulphur species, to surrounding culture medium in association with a loss of membrane integrity
15 by stressed cells or as a result of viral lysis. Hughes et al. (2011) also reported studies with cultures
16 of *Prochlorococcus marinas* in which accumulation of CH₃I commenced when cultures became
17 senescent. We note that significant iodocarbon accumulation in Bedford Basin was confined to
18 summertime when DIN was depleted (see Fig. 3b) and when cells may have been stressed or
19 subject to viral lysis, perhaps similar to later stages of batch culture experiments.

20 We therefore hypothesize that seasonal nitrate drawdown leads to increased supply of iodide to
21 surface waters which can, in turn, lead to increased formation of iodine atoms, HOI and I₂ as
22 precursors for iodocarbon formation by both photochemical and haloform reaction pathways
23 (Martino et al., 2009; Moore and Zafiriou, 1994). Whereas the supply of iodide may be one key

1 control, it is likely that variations in light intensity and water temperature also contribute to the
2 overall seasonality of the production rate of CH₃I (e.g. through temperature influence on reaction
3 kinetics). For example, light can influence formation of CH₃I directly (e.g. Moore and Zafiriou,
4 1994; Richter and Wallace, 2004). Light can also influence iodocarbon production indirectly, for
5 example by producing oxidants such as H₂O₂ to promote oxidation of iodide by haloperoxidases
6 (Hill and Manley, 2009) or by altering the quality of dissolved organic matter. The time-series of
7 CH₂I₂ and CH₂ClI from very shallow (< 4 m), nearshore waters of the Kattegat, Sweden (Klick,
8 1992) and the Baltic Sea, Germany (Orlikowska and Schulz-Bull, 2009) showed peaks in April/
9 May and again in September/October, with low concentrations throughout summer. This contrasts
10 with the deeper water columns of Bedford Basin, Funka Bay and the English Channel where
11 concentrations remain elevated throughout summer. This likely reflects dominance of photolytic
12 loss over production within very shallow water columns exposed to summertime light intensities
13 and long periods of daylight. Sub-surface production coupled with vertical mixing may explain
14 the summertime persistence in deeper water columns.

15 In addition to the broad seasonal variation, a number of maxima with duration of ca. 1 month, were
16 observed, and appear similar to short-period fluctuations observed in the English Channel time-
17 series (Archer et al., 2007). There does not appear to be any consistent pattern linking the maxima
18 and minima of the three compounds in the two studies, so that the underlying causes for these
19 shorter period variations are unclear.

20

21 4.3.2 Interannual variability

22 The Bedford Basin time-series is unique in having high temporal resolution sampling (weekly)
23 over three annual cycles which allows interannual variability to be examined for the first time. The

1 most obvious interannual difference was in the behavior of CH₃I. In particular, 2016 was markedly
2 different in that only a single peak was observed in late August, whereas the summers of 2015 and
3 2017 were marked by 3-4 quasi-periodic, multi-week maxima. As noted already, the English
4 Channel time-series of CH₃I did not exhibit this behavior. The shallow-water time-series of CH₃I
5 in the Kiel Fjord and coastal Baltic Sea (Orlikowska and Schulz-Bull, 2009; Shi et al., 2014b) also
6 did not exhibit this type of variability. Because the cause of the periodicity itself is not understood
7 or explained, discussion of reasons for its interannual variation must be highly speculative. One
8 clear difference of 2016 relative to the other two years, was the lower summertime precipitation
9 and associated lack of near-surface salinity stratification. The temporal behavior of CH₃I in 2016
10 might therefore be related to altered near-surface mixing dynamics within Bedford Basin, or
11 alternatively, to decreased delivery of key precursors (e.g. DOM) from land via rivers and
12 wastewater.

13

14 4.4 Vertical distributions and subsurface temporal variability

15 Fig. 4 shows the near-surface concentration variations of the VOIs. For CH₃I, concentrations were
16 almost always uniform between 1, 5 and 10 m. For CH₂ClI, the concentrations at 1 and 5m were
17 usually very similar (average difference -4.1 %; median -2.5 %), however concentrations at 10m
18 depth were noticeably lower for periods of time. For CH₂I₂, the highest concentrations were
19 observed at a depth of either 5 or 10 m, with concentrations at 5 m occasionally peaking at very
20 high levels (e.g. 250-350 pmol L⁻¹) for short periods (less than one week). Concentrations at 1 m
21 were almost always lower than at 5 m, with the percentage reduction relative to 5 m averaging 52 %
22 in summer. Concentrations at 10 m, on the other hand, were generally the same or higher as those
23 measured at 5 m (with the exception of the previously mentioned, short-lived peaks).

1 These results are consistent with earlier studies of vertical profiles in the open ocean (e.g. (Moore
2 and Tokarczyk, 1993; Yamamoto et al., 2001)) as well as with model predictions (Jones et al.,
3 2010; Martino et al., 2006). In particular, our results are consistent with the quantitative predictions
4 of a mixed-layer model (Jones et al., 2010) that CH₂ClI would typically be near-uniform within
5 the upper 6 m of the water column, whereas photolytic decay could remove up to 100 % of the
6 CH₂I₂ over that depth range, depending on time of day and conditions.

7

8 4.5 Temporal variability in near-bottom water (60 m)

9 The time-series of VOIs in near-bottom waters (60 m) are presented in detail in Fig. 9a,b,c, with
10 specific events labelled 1 through 9. Variability was generally of lower amplitude than in surface
11 waters, except for CH₃I during the winter of 2015-2016 (Fig. 4d). From June to December 2015,
12 [CH₃I] increased steadily (concentration change, $\Delta C = 20 \text{ pmol L}^{-1}$) (event 1 to 3; Fig. 9a),
13 exceeding surface water concentrations from October 2015 until the end of March 2016. No
14 comparable increase was observed during 2016 (Fig. 9b), and a smaller increase ($\Delta C = 8 \text{ pmol L}^{-1}$)
15 was confined to the early summer of 2017 (Fig. 9c).

16 Concentrations of CH₂ClI remained almost constant at $<5 \text{ pmol L}^{-1}$ throughout, with the notable
17 exception of abrupt (<1 week) increases in May and November 2016 (events 4 and 5; Fig. 9b) and
18 December 2017 (event 9; Fig. 9c). These increases ($\Delta C = 2\text{-}5 \text{ pmol L}^{-1}$) coincided with sudden
19 increases of salinity (and O₂) and reflect intrusion of saltier, near-surface waters from offshore,
20 rather than local production. The subsequent concentration declines reflect loss due to mixing or,
21 more likely, reaction and/or microbial degradation within the water column and sediments. The
22 same three intrusions also drove abrupt increases of CH₂I₂ with amplitude ca. 1.5 – 2 times higher
23 than those for CH₂ClI, consistent with near-surface concentration ratios (see section 3.2). However,

1 CH₂I₂ also showed higher-amplitude variations unrelated to the bottom water intrusions (see
2 below).

3 The increase of CH₃I from June through October 2015 (event 1 through 3; Fig. 9a), paralleled a
4 steady decline in oxygen, suggesting that production was linked to degradation of organic matter.
5 The accumulation rate of ca. 0.06 pmol L⁻¹ day⁻¹ was 20 times smaller than typical P_{net} for CH₃I
6 in surface waters (see section 3.4). The increase appears consistent with results from short-term
7 (3-day) incubation experiments with biogenic marine aggregates reported by Hughes et al. (2008)
8 in which concentrations of mono-iodinated iodocarbons, including CH₃I, increased but with no
9 corresponding increase in dihalogenated compounds. Their results suggested alkylation of
10 inorganic iodine or breakdown of higher molecular mass organohalogens as production pathways
11 and, following Amachi et al. (2001), they suggested that microbial degradation increased the
12 supply of precursors.

13 However, as O₂ concentrations declined further from October through late December (event 2 to
14 3; Fig. 9a), the concentration of CH₃I stabilized and CH₂I₂ concentration increased markedly from
15 2 to 12 pmol L⁻¹. From January through April 2016, CH₃I levels decreased (following event 3; Fig.
16 9a,b), in concert with increasing O₂ concentrations and decreasing salinity, reflecting the effects
17 of progressive vertical mixing with overlying waters which had lower CH₃I concentrations. Over
18 this same period, CH₂I₂ concentrations at 60 m remained almost constant (Fig. 9a, b) due to the
19 smaller vertical concentration gradient, until increasing due to an intrusion (event 4). This was
20 followed by a gradual decrease over summer months, in parallel with the seasonal decrease of O₂
21 (fig 9b).

22 The data from 2015 and 2017 are suggestive of a “switch” of production mechanism from an
23 alkylation pathway producing mono-iodinated compounds (CH₃I) to a haloform-type reaction

1 producing CH_2I_2 . The “switch” took place in October 2015 (event 2; Fig. 9a), when oxygen
2 concentrations dropped below $90 \mu\text{mol kg}^{-1}$, although whether the switch was related to redox
3 conditions in the water column or sediments, speciation and availability of iodine, or availability
4 of suitable organic precursors and/or enzymes cannot be determined.

5 There was almost no near-bottom iodocarbon production during 2016 (Fig. 9b), and therefore no
6 “switch”, for reasons that are not clear given that O_2 declined through summer and fall, until
7 interrupted by an intrusion in November (event 5; Fig. 9b). We speculate that the lack of production
8 in near-bottom water might be linked to the relatively short period of CH_3I production in near-
9 surface waters during that year (fig 4a).

10 In 2017, there was moderate sub-surface production of CH_3I , associated with O_2 consumption
11 (April through July; event 6 to 7), and, again, an apparent “switch” to CH_2I_2 production marked
12 by plateauing of CH_3I concentrations (event 7) at the same time as CH_2I_2 concentrations started to
13 increase (Fig. 9c). This was followed by a subsequent decrease to background levels over a period
14 of about a month. The apparent “switch” in production took place earlier in the year and at higher
15 O_2 concentrations ($175 \mu\text{mol kg}^{-1}$) than in 2015.

16 However close inspection of Fig. 2 shows that the plateauing of CH_3I in near-bottom waters (event
17 7) coincided with the appearance of a mid-depth intrusion of saltier water (as denoted by the 31
18 salinity contour; see blue circled area in Fig. 2). The same period (between events 7 and 8) was
19 marked at 60m by a change from declining to increasing salinity, reduction in the rate of oxygen
20 concentration decline (Fig. 9c) and an increase in the rate of warming (not shown). The mid-depth
21 salinity maximum in Bedford Basin must reflect intrusion of saltier water from offshore. The
22 subsequent trends in temperature, salinity and dissolved oxygen at 60m, between events 7 and 8
23 (Fig. 9c), are consistent with mixing of pre-existing near-bottom water with this intrusion. It is

1 therefore possible that mixing contributed in some way to the increase of CH_2I_2 , plateauing of
2 CH_3I concentrations as well as a small but significant increase in CH_2CII ($\Delta C=1-2 \text{ pmol L}^{-1}$) which
3 all occurred at the same time.

4 At the end of this period, in mid-August (event 8), the rate of warming and salinity increase at 60
5 m decreased again and the rate of oxygen decline increased (Fig. 9c), suggesting that the
6 intrusion's impact had lessened. At this time, CH_2I_2 and CH_3I concentrations started to return to
7 background levels with estimated half-life, assuming 1st order kinetics, of ca. 65 days (CH_2I_2) and
8 14 days (CH_3I). A decrease in $[\text{CH}_2\text{CII}]$ started about a month later with 1st order half-life of ca.
9 70 days. Similar rates of decline of $[\text{CH}_2\text{CII}]$ and $[\text{CH}_2\text{I}_2]$ were observed following sudden
10 concentration increases associated with other intrusions, discussed earlier.

11 This very detailed discussion of the temporal variability emphasizes that a variety of physical and
12 biogeochemical mechanisms can contribute to interannual, seasonal, and short-term variability of
13 the three iodocarbons. The high amplitude variability observed in Bedford Basin could prove
14 useful for validation of models representing complex iodine cycling as well as physical mixing
15 dynamics. However, separation of multiple potential contributing factors and processes underlying
16 temporal variability may require a data set with higher vertical resolution and, ideally, a seasonally-
17 resolved time-series of experiments (compare Shi et al., 2014a).

18

19 4.6 Sea-to-air fluxes

20 The temporal variation of the sea-to-air flux of I_{org} and the relative contribution from the three
21 iodocarbons are shown in Fig. 5 and Table 3. Similar to the findings of Archer et al. (2007), air-
22 side resistance leads to significant reductions in calculated, annual average fluxes for CH_2CII and
23 CH_2I_2 of 10% and 24%, respectively, relative to calculations when it is ignored. The study by

1 Shimizu et al. (2017) did not consider air-side resistance, so Table 5 presents both their original
2 reported fluxes, as well as fluxes adjusted for its likely impact based on our study and that of
3 Archer et al. (2007). The following discussion makes use of the adjusted fluxes.

4 Consistent with earlier time-series (excluding those from very shallow waters, see section 4.2), the
5 sea-to-air flux of iodocarbons is generally highest in summer/fall. However, high wintertime fluxes
6 are also possible, as seen in 2017 when there was a large efflux of CH_2I_2 (averaging 9.1 nmol m^{-2}
7 d^{-1} ; Table 3), due to both strong winds and relatively high concentrations. The fluxes of CH_3I and
8 CH_2CII , on the other hand, were always higher in summer/fall (ca. 3-5 times and 10 times higher,
9 respectively). Similar findings were presented by Shimizu et al. (2017) with the total iodine flux
10 in Funka Bay in summer being > 4 times that in winter.

11 Our estimated emissions of CH_3I ($8.4 \text{ nmol m}^{-2} \text{ d}^{-1}$, Table 5) are in the range calculated previously
12 for coastal and continental shelf water in similar latitudes (11.9 and $7.7 \text{ nmol m}^{-2} \text{ d}^{-1}$; Archer et
13 al., 2007; Shimizu et al., 2017 respectively). The average flux of CH_3I reported by Jones et. al
14 (2010), from the west of Ireland, was 4 times higher but based on a sampling period of only 1
15 month during summer. Sea-to-air fluxes of CH_2CII from Funka Bay and English Channel were
16 similar to our calculated fluxes from Bedford Basin. However the highest variation is observed in
17 the annual averaged flux of CH_2I_2 , ranging from $3.5 \text{ nmol m}^{-2} \text{ d}^{-1}$ (the west English Channel), 10.3
18 $\text{nmol m}^{-2} \text{ d}^{-1}$ (Bedford Basin) and $12.6 \text{ nmol m}^{-2} \text{ d}^{-1}$ (Funka Bay, Japan). The total, annual I_{org} sea-
19 to-air flux from Bedford Basin averaged $46.7 \text{ nmol m}^{-2} \text{ d}^{-1}$, which was approximately 5 times larger
20 than the flux due to CH_3I alone. The total annual flux was similar between all three locations.

21 Fig. 5 and Table 3 show that the total I_{org} flux is subject to significant interannual variability, which
22 could not be assessed by the earlier studies. Notably, the I_{org} flux in 2016 was ca. 2 times smaller
23 than in 2015 and 2017. A comparison of wind-speeds and concentrations showed that although

1 both factors, the influence of wind speed was dominant, due to winds during summer/fall of 2016
2 being 1-2 m s⁻¹ lower.

3

4 4.7 Production rate of CH₃I

5 The annual mean production rate (P_{net}) of CH₃I in this study, estimated using equation 1, was 1.0
6 pmol L⁻¹ day⁻¹ (ranging from -1.6 to 8.5 pmol L⁻¹ day⁻¹, see section 3.4 and Fig. 6). This is
7 comparable with the global average production rate estimated by Stemmler et al. (2013) (1.64
8 pmol L⁻¹ day⁻¹), for which 70% was produced via a photochemical mechanism. Based on data
9 presented by Archer et al. (2007), the annual mean production rate of CH₃I in the western English
10 Channel was ca. 2 pmol L⁻¹ day⁻¹ (range: -0.2 to 6 pmol L⁻¹ day⁻¹). Here it should be noted, that
11 their “minimum gross production rate” is equivalent to P_{net} in this study and in Shi et al. (2014a).
12 In contrast, Shi et al. (2014b) estimated a considerably lower annual mean net production rate in
13 the Kiel Fjord of ca. 0.1 pmol L⁻¹ day⁻¹ (maximum of 0.8 pmol L⁻¹ day⁻¹). The maximum production
14 rates from the Kiel Fjord study were based on monthly average concentrations, and therefore
15 expected to be smaller. However, Shi et al. (2014a) also conducted weekly incubation experiments
16 which gave *in vitro* values of P_{net} which were closely comparable with the field-based estimates.
17 The lower values of P_{net} in the Kiel Fjord compared with both Bedford Basin and the English
18 Channel must reflect either differences in gross production (e.g. due to differences in the supply
19 of precursors and reactants such as iodide) or differences in other, uncharacterized losses. An
20 additional, poorly characterized loss process, possibly microbial degradation, was in fact observed
21 in the Kiel Fjord incubation experiments (Shi et al., 2014a). On the other hand, incubation
22 experiments conducted with additions of labelled methyl iodide (¹³CD₃I) to Bedford Basin surface
23 waters (data not shown) during the course of this study showed no such losses. We therefore

1 hypothesize that the lower P_{net} in Kiel Fjord is a result of higher microbial degradation of CH_3I in
2 that very shallow (<12 m), nearshore environment.

3

4 5. Conclusions, Implications and Further Work

5 The 3-year time-series of weekly iodocarbon concentrations from Bedford Basin shows overall
6 seasonality similar to that observed in coastal time-series from both the English Channel and Funka
7 Bay, Japan. There was no mid-summer minimum in the concentration of polyiodinated compounds
8 as observed in some time-series from very shallow water (<10m), which likely reflects dominance
9 of photolytic decay in such shallow water columns. Interannual variability in near-surface water
10 concentrations was particularly pronounced for CH_3I , with only a single, short-lived concentration
11 maximum observed in 2016, possibly as a result of anomalously low rainfall and consequently
12 reduced supply of terrestrial organic matter during that summer.

13 Based on the time-series as well as published lab studies, we hypothesize that seasonal, near-
14 surface production of iodocarbons is linked to accelerated reduction of iodate to iodide under post-
15 bloom conditions, following disappearance of nutrients and possibly also influenced by water
16 temperature. The observed vertical variation of CH_2I_2 and CH_2ClI is consistent with the more rapid
17 photolysis of CH_2I_2 .

18 The average annual sea-to-air flux of total volatile organic iodine ($46.7 \text{ nmol m}^{-2} \text{ d}^{-1}$) is almost
19 identical to that observed in Funka Bay, Japan, and the English Channel. The polyiodinated
20 compounds contributed ca. 80 % of the total flux which was similar to that in the other two time-
21 series and confirms that the sea-to-air flux of polyiodinated compounds dominates in coastal
22 waters. The fluxes were variable on interannual timescales (factor of 2) as a result, mainly, of
23 wind-speed variability.

1 The near-bottom water (60m) time-series was impacted by episodic intrusions of water from
2 offshore and showed evidence for CH₃I production associated with decay of organic matter, albeit
3 with a production rate more than an order of magnitude lower than in surface waters. The time-
4 series showed evidence for a possible “switch” from CH₃I production (e.g. by alkylation of organic
5 matter) to production of CH₂I₂ (e.g. by a haloform type reaction), after periods of about 1 month.
6 The very high amplitude concentration variations encountered in Bedford Basin, coupled with its
7 relative accessibility for high-frequency sampling and constrained, yet variable, physical
8 exchanges make Bedford Basin a useful location to investigate iodine cycling. To-date, the
9 complexity of iodine biogeochemistry has hindered progress towards understanding the controls
10 on spatial and temporal fluxes of iodine between the ocean and atmosphere. We suggest that
11 progress can now be made through more comprehensive sampling (higher vertical resolution and
12 inclusion of inorganic iodine speciation measurement), coupled to a biogeochemical model of
13 Bedford Basin that includes iodine chemistry (e.g. Stemmler et al, 2013) and a time-series of
14 experimental studies conducted in the context of the time-series (see Shi et al., 2014a). In other
15 words, Bedford Basin may provide an ideal location and time-series upon which to base a multi-
16 investigator campaign to understand environmental controls on volatile iodine cycling and
17 improve its representation in models.

18

19 Acknowledgments

20 This work was funded by the Canada Excellence Research Chair in Ocean Science and Technology
21 at Dalhousie University. Sampling of the Bedford Basin time-series was supported by MEOPAR
22 Observation Core, Department of Fisheries and Ocean, Canada (DFO) and Bedford Basin
23 Monitoring Program (BBMP) (<http://www.bio.gc.ca/science/monitoring-monitorage/bbmp->

1 pobb/bbmp-pobb-en.php). The authors thank Richard Davis, Anna Haverstock and the crew of the
2 Sigma-T. Assistance and guidance in the laboratory from Claire Normandeau and Liz Kerrigan
3 are also acknowledged.

4

5 Reference

6 Amachi, S., Kamagata, Y., Kanagawa, T. and Muramatsu, Y.: Bacteria mediate methylation of
7 iodine in marine and terrestrial environments, *Applied and environmental microbiology*,
8 67(6), 2718–2722, 2001.

9 Archer, S. D., Goldson, L. E., Liddicoat, M. I., Cummings, D. G. and Nightingale, P. D.: Marked
10 seasonality in the concentrations and sea-to-air flux of volatile iodocarbon compounds in
11 the western English Channel, *Journal of Geophysical Research: Oceans*, 112(C8), C08009,
12 doi:10.1029/2006JC003963, 2007.

13 Bluhm, K., Croot, P. L., Huhn, O., Rohardt, G. and Lochte, K.: Distribution of iodide and iodate
14 in the Atlantic sector of the southern ocean during austral summer, *Deep Sea Research*
15 Part II: Topical Studies in Oceanography, 58(25), 2733–2748, 2011.

16 Brownell, D. K., Moore, R. M. and Cullen, J. J.: Production of methyl halides by *Prochlorococcus*
17 and *Synechococcus*, *Global Biogeochemical Cycles*, 24(2), GB2002, 2010.

18 Buckley, D. E. and Winters, G. V: Geochemical characteristics of contaminated surficial
19 sediments in Halifax Harbour: impact of waste discharge, *Canadian Journal of Earth*
20 *Sciences*, 29(12), 2617–2639, 1992.

21 Burt, W. J., Thomas, H., Fennel, K. and Horne, E.: Sediment-water column fluxes of carbon,
22 oxygen and nutrients in Bedford Basin, Nova Scotia, inferred from ²²⁴Ra measurements,

1 Biogeosciences, 10(1), 53–66, doi:10.5194/bg-10-53-2013, 2013.

2 Carpenter, L. J.: Iodine in the marine boundary layer, *Chemical reviews*, 103(12), 4953–4962,
3 2003.

4 Carpenter, L. J., Malin, G. and Liss, P. S.: Novel biogenic iodine-containing trihalomethanes and
5 other, *Global Biogeochemical Cycles*, 14(4), 1191–1204, 2000.

6 Carpenter, L. J., MacDonald, S. M., Shaw, M. D., Kumar, R., Saunders, R. W., Parthipan, R.,
7 Wilson, J. and Plane, J. M. C.: Atmospheric iodine levels influenced by sea surface
8 emissions of inorganic iodine, *Nature Geoscience*, 6(2), 108, 2013.

9 Carpenter, L. J., Reimann, S., Burkholder, J. B., Clerbaux, C., Hall, B. D., Hossaini, R., Laube, J.
10 C., Yvon-Lewis, S. A., Engel, A. and Montzka, S. A.: Update on ozone-depleting substances
11 (ODSs) and other gases of interest to the Montreal protocol, *Scientific assessment of*
12 *ozone depletion: 2014*, 1, 2014.

13 Davis, D., Crawford, J., Liu, S., McKeen, S., Bandy, A., Thornton, D., Rowland, F. and Blake, D.:
14 Potential impact of iodine on tropospheric levels of ozone and other critical oxidants,
15 *Journal of Geophysical Research: Atmospheres*, 101(D1), 2135–2147, 1996.

16 Duce, R. A., Liss, P. S., Merrill, J. T., Atlas, E. L., Buat-Menard, P., Hicks, B. B., Miller, J. M.,
17 Prospero, J. M., Arimoto, R., Church, T. M., Ellis, W., Galloway, J. N., Hansen, L., Jickells, T.
18 D., Knap, A. H., Reinhardt, K. H., Schneider, B., Soudine, A., Tokos, J. J., Tsunogai, S.,
19 Wollast, R. and Zhou, M.: The atmospheric input of trace species to the world ocean,
20 *Global Biogeochemical Cycles*, 5(3), 193–259, doi:10.1029/91GB01778, 1991.

21 Elliott, S. and Rowland, F. S.: Nucleophilic substitution rates and solubilities for methyl halides
22 in seawater, *Geophysical Research Letters*, 20(11), 1043–1046, 1993.

- 1 Fuse, H., Inoue, H., Murakami, K., Takimura, O. and Yamaoka, Y.: Production of free and
2 organic iodine by *Roseovarius* spp., *FEMS Microbiology Letters*, 229(2), 189–194,
3 doi:10.1016/S0378-1097(03)00839-5, 2003.
- 4 Garland, J. A., Elzerman, A. W. and Penkett, S. A.: The mechanism for dry deposition of ozone
5 to seawater surfaces, *Journal of Geophysical Research: Oceans*, 85(C12), 7488–7492,
6 1980.
- 7 Giese, B., Laturnus, F., Adams, F. C. and Wiencke, C.: Release of Volatile Iodinated C1– C4
8 Hydrocarbons by Marine Macroalgae from Various Climate Zones, *Environmental science*
9 & technology, 33(14), 2432–2439, 1999.
- 10 Groszko, W. M.: An estimate of the global air-sea flux of methyl chloride, methyl bromide, and
11 methyl iodide, PhD Thesis, Dalhousie University., 1999.
- 12 Hepach, H., Quack, B., Tegtmeier, S., Engel, A., Bracher, A., Fuhlbrügge, S., Galgani, L., Atlas, E.
13 L., Lampel, J., Frieß, U. and Krüger, K.: Biogenic halocarbons from the Peruvian upwelling
14 region as tropospheric halogen source, *Atmospheric Chemistry and Physics*, 16(18),
15 12219–12237, doi:10.5194/acp-16-12219-2016, 2016.
- 16 Hill, V. L. and Manley, S. L.: Release of reactive bromine and iodine from diatoms and its
17 possible role in halogen transfer in polar and tropical oceans, *Limnology and*
18 *Oceanography*, 54(3), 812–822, doi:10.4319/lo.2009.54.3.0812, 2009.
- 19 Hughes, C., Malin, G., Turley, C. M., Keely, B. J. and Nightingale, P. D.: The production of volatile
20 iodocarbons by biogenic marine aggregates, *Limnology and Oceanography*, 53(2), 867–
21 872, 2008.
- 22 Hughes, C., Franklin, D. J. and Malin, G.: Iodomethane production by two important marine

1 cyanobacteria: *Prochlorococcus marinus* (CCMP 2389) and *Synechococcus* sp.(CCMP
2 2370), *Marine Chemistry*, 125(1–4), 19–25, 2011.

3 Jones, C. E. and Carpenter, L. J.: Solar photolysis of CH₂I₂, CH₂ICl, and CH₂I₂Br in water,
4 saltwater, and seawater, *Environmental science & technology*, 39(16), 6130–6137, 2005.

5 Jones, C. E. and Carpenter, L. J.: Chemical destruction of CH₃I, C₂H₅I, 1-C₃H₇I, and 2-C₃H₇I in
6 saltwater, *Geophysical Research Letters*, 34(13), 1–6, doi:10.1029/2007GL029775, 2007.

7 Jones, C. E., Hornsby, K. E., Dunk, R. M., Leigh, R. J. and Carpenter, L. J.: Coastal measurements
8 of short-lived reactive iodocarbons and bromocarbons at Roscoff, Brittany during the
9 RHaMBLe campaign, *Atmospheric Chemistry and Physics*, 9(22), 8757–8769,
10 doi:10.5194/acp-9-8757-2009, 2009.

11 Jones, C. E., Hornsby, K. E., Sommariva, R., Dunk, R. M., Von Glasow, R., McFiggans, G. and
12 Carpenter, L. J.: Quantifying the contribution of marine organic gases to atmospheric
13 iodine, *Geophysical Research Letters*, 37(18), L18804, 2010.

14 Kerrigan, E. A., Kienast, M., Thomas, H. and Wallace, D. W. R.: Using oxygen isotopes to
15 establish freshwater sources in Bedford Basin, Nova Scotia, a Northwestern Atlantic fjord,
16 *Estuarine, Coastal and Shelf Science*, 199, 96–104, 2017.

17 Klick, S.: Seasonal variations of biogenic and anthropogenic halocarbons in seawater from a
18 coastal site, *Limnology and oceanography*, 37(7), 1579–1585, 1992.

19 Kurihara, M. K., Kimura, M., Iwamoto, Y., Narita, Y., Ooki, A., Eum, Y. J., Tsuda, A., Suzuki, K.,
20 Tani, Y., Yokouchi, Y., Uematsu, M. and Hashimoto, S.: Distributions of short-lived
21 iodocarbons and biogenic trace gases in the open ocean and atmosphere in the western
22 North Pacific, *Marine Chemistry*, 118(3–4), 156–170,

1 doi:10.1016/j.marchem.2009.12.001, 2010.

2 Li, B.: Changes in Planktonic Microbiota, in Preserving the enviroment of Halifax Harbour,
3 edited by L. Williamm K, W., G. Turner, and A. Ducharme, pp. 105–121., 2001.

4 Li, W. K. W.: Annual average abundance of heterotrophic bacteria and *Synechococcus* in
5 surface ocean waters, *Limnology and oceanography*, 43(7), 1746–1753, 1998.

6 Liss, P. S. and Slater, P. G.: Flux of Gases across the Air-Sea Interface, *Nature*, 247(5438), 181–
7 184, doi:10.1038/247181a0, 1974.

8 Mahajan, A. S., Plane, J. M. C., Oetjen, H., Mendes, L., Saunders, R. W., Saiz-Lopez, A., Jones,
9 C. E., Carpenter, L. J. and McFiggans, G. B.: Measurement and modelling of tropospheric
10 reactive halogen species over the tropical Atlantic Ocean, *Atmospheric Chemistry and*
11 *Physics*, 10(10), 4611–4624, 2010.

12 Mahajan, A. S., Gómez Martín, J. C., Hay, T. D., Royer, S.-J., Yvon-Lewis, S., Liu, Y., Hu, L.,
13 Prados-Roman, C., Ordóñez, C. and Plane, J. M. C.: Latitudinal distribution of reactive
14 iodine in the Eastern Pacific and its link to open ocean sources, *Atmospheric Chemistry*
15 *and Physics*, 12(23), 11609–11617, 2012.

16 Manley, S. L. and de la Cuesta, J. L.: Methyl iodide production from marine phytoplankton
17 cultures, *Limnology and Oceanography*, 42(1), 142–147, 1997.

18 Martino, M., Liss, P. S. and Plane, J. M. C.: The Photolysis of Dihalomethanes in Surface
19 Seawater, *Environmental Science & Technology*, 39(18), 7097–7101,
20 doi:10.1021/es048718s, 2005.

21 Martino, M., Liss, P. S. and Plane, J.: Wavelength-dependence of the photolysis of
22 diiodomethane in seawater, *Geophysical research letters*, 33(6), L06606, 2006.

- 1 Martino, M., Mills, G. P., Woeltjen, J. and Liss, P. S.: A new source of volatile organoiodine
2 compounds in surface seawater, *Geophysical Research Letters*, 36(1), L01609,
3 doi:10.1029/2008GL036334, 2009.
- 4 McFiggans, G., Plane, J., Allan, B. J., Carpenter, L. J., Coe, H. and O'Dowd, C.: A modeling study
5 of iodine chemistry in the marine boundary layer, *Journal of Geophysical Research:*
6 *Atmospheres*, 105(D11), 14371–14385, 2000.
- 7 McFiggans, G., Coe, H., Burgess, R., Allan, J., Cubison, M., Alfarra, M. R., Saunders, R., Saiz-
8 Lopez, A., Plane, J. M. C. and Wevill, D.: Direct evidence for coastal iodine particles from
9 *Laminaria macroalgae*—linkage to emissions of molecular iodine, *Atmospheric Chemistry*
10 *and Physics*, 4(3), 701–713, 2004.
- 11 Moore, R. M. and Tokarczyk, R.: Volatile biogenic halocarbons in the northwest Atlantic, *Global*
12 *Biogeochemical Cycles*, 7(1), 195–210, 1993.
- 13 Moore, R. M. and Zafiriou, O. C.: Photochemical production of methyl iodide in seawater,
14 *Journal of Geophysical Research: Atmospheres*, 99(D8), 16415–16420, 1994.
- 15 Moore, R. M., Geen, C. E. and Tait, V. K.: Determination of Henry's law constants for a suite of
16 naturally occurring halogenated methanes in seawater, *Chemosphere*, 30(6), 1183–1191,
17 1995.
- 18 Mössinger, J. C., Shallcross, D. E. and Cox, R. A.: UV–VIS absorption cross-sections and
19 atmospheric lifetimes of CH₂Br₂, CH₂I₂ and CH₂BrI, *Journal of the Chemical Society,*
20 *Faraday Transactions*, 94(10), 1391–1396, 1998.
- 21 Nightingale, P. D., Malin, G., Law, C. S., Watson, A. J., Liss, P. S., Liddicoat, M. I., Boutin, J. and
22 Upstill-Goddard, R. C.: In situ evaluation of air-sea gas exchange parameterizations using

1 novel conservative and volatile tracers, *Global Biogeochemical Cycles*, 14(1), 373–387,
2 2000.

3 O’Dowd, C. D., Jimenez, J. L., Bahreini, R., Flagan, R. C., Seinfeld, J. H., Hameri, K., Pirjola, L.,
4 Kulmala, M., Jennings, S. G. and Hoffmann, T.: Marine aerosol formation from biogenic
5 iodine emissions, *Nature*, 417(6889), 632–636 [online] Available from:
6 <http://dx.doi.org/10.1038/nature00775>, 2002.

7 Orlikowska, A. and Schulz-Bull, D. E.: Seasonal variations of volatile organic compounds in the
8 coastal Baltic Sea, *Environmental Chemistry*, 6(6), 495–507, doi:10.1071/EN09107, 2009.

9 Orlikowska, A., Stolle, C., Pollehne, F., Jürgens, K. and Schulz-Bull, D. E.: Dynamics of
10 halocarbons in coastal surface waters during short term mesocosm experiments,
11 *Environmental Chemistry*, 12(4), 515–525, doi:10.1071/EN14204, 2015.

12 Rasmussen, R. A., Khalil, M. A. K., Gunawardena, R. and Hoyt, S. D.: Atmospheric methyl iodide
13 (CH₃I), *Journal of Geophysical Research: Oceans*, 87(C4), 3086–3090, 1982.

14 Rattigan, O., Shallcross, D. and Anthony Cox, R.: UV absorption cross-sections and
15 atmospheric photolysis rates of CF₃I, CH₃I, C₂H₅I and CH₂ICl, *Journal of the Chemical*
16 *Society, Faraday Transactions*, 93(16), 2839–2846, 1997.

17 Richter, U. and Wallace, D. W. R.: Production of methyl iodide in the tropical Atlantic Ocean,
18 *Geophysical Research Letters*, 31(23), L23S03, doi:10.1029/2004GL020779, 2004.

19 Saiz-Lopez, A. and Von Glasow, R.: Reactive halogen chemistry in the troposphere, *Chemical*
20 *Society Reviews*, 41(19), 6448, doi:10.1039/c2cs35208g, 2012.

21 Schall, C., Laturnus, F. and Heumann, K. G.: Biogenic volatile organoiodine and organobromine
22 compounds released from polar macroalgae, *Chemosphere*, 28(7), 1315–1324,

1 doi:10.1016/0045-6535(94)90076-0, 1994.

2 Shan, S., Sheng, J., Thompson, K. R. and Greenberg, D. A.: Simulating the three-dimensional
3 circulation and hydrography of Halifax Harbour using a multi-nested coastal ocean
4 circulation model, *Ocean Dynamics*, 61(7), 951–976, 2011.

5 Shi, Q., Petrick, G., Quack, B., Marandino, C. and Wallace, D. W. R.: A time series of incubation
6 experiments to examine the production and loss of CH₃I in surface seawater, *Journal of*
7 *Geophysical Research Oceans*, (2), 1022–1037, doi:10.1002/2013JC009415, 2014a.

8 Shi, Q., Petrick, G., Quack, B., Marandino, C. and Wallace, D.: Seasonal variability of methyl
9 iodide in the Kiel Fjord, *Journal of Geophysical Research: Oceans*, 119(3), 1609–1620,
10 doi:10.1002/2013JC009328, 2014b.

11 Shimizu, Y., Ooki, A., Onishi, H., Takatsu, T., Tanaka, S., Inagaki, Y., Suzuki, K., Kobayashi, N.,
12 Kamei, Y. and Kuma, K.: Seasonal variation of volatile organic iodine compounds in the
13 water column of Funka Bay, Hokkaido, Japan, *Journal of Atmospheric Chemistry*, 74(2),
14 205–225, 2017.

15 Smythe-Wright, D., Boswell, S. M., Breithaupt, P., Davidson, R. D., Dimmer, C. H. and Eiras Diaz,
16 L. B.: Methyl iodide production in the ocean: Implications for climate change, *Global*
17 *Biogeochemical Cycles*, 20(3), GB3003, 2006.

18 Solomon, S., Garcia, R. R. and Ravishankara, A. R.: On the role of iodine in ozone depletion,
19 *Journal of Geophysical Research: Atmospheres*, 99(D10), 20491–20499, 1994.

20 Stemmler, I., Rothe, M., Hense, I. and Hepach, H.: Numerical modelling of methyl iodide in the
21 eastern tropical Atlantic, *Biogeosciences (BG)*, 10(6), 4211–4225, 2013.

22 Stemmler, I., Hense, I., Quack, B. and Maier-Reimer, E.: Methyl iodide production in the open

1 ocean, Biogeosciences (BG), 11(16), 4459–4476, 2014.

2 Tegtmeier, S., Krüger, K., Quack, B., Atlas, E., Blake, D. R., Bönisch, H., Engel, A., Hepach, H.,
3 Hossaini, R. and Navarro, M. A.: The contribution of oceanic methyl iodide to
4 stratospheric iodine, Atmospheric Chemistry and Physics, 13(23), 11869–11886, 2013.

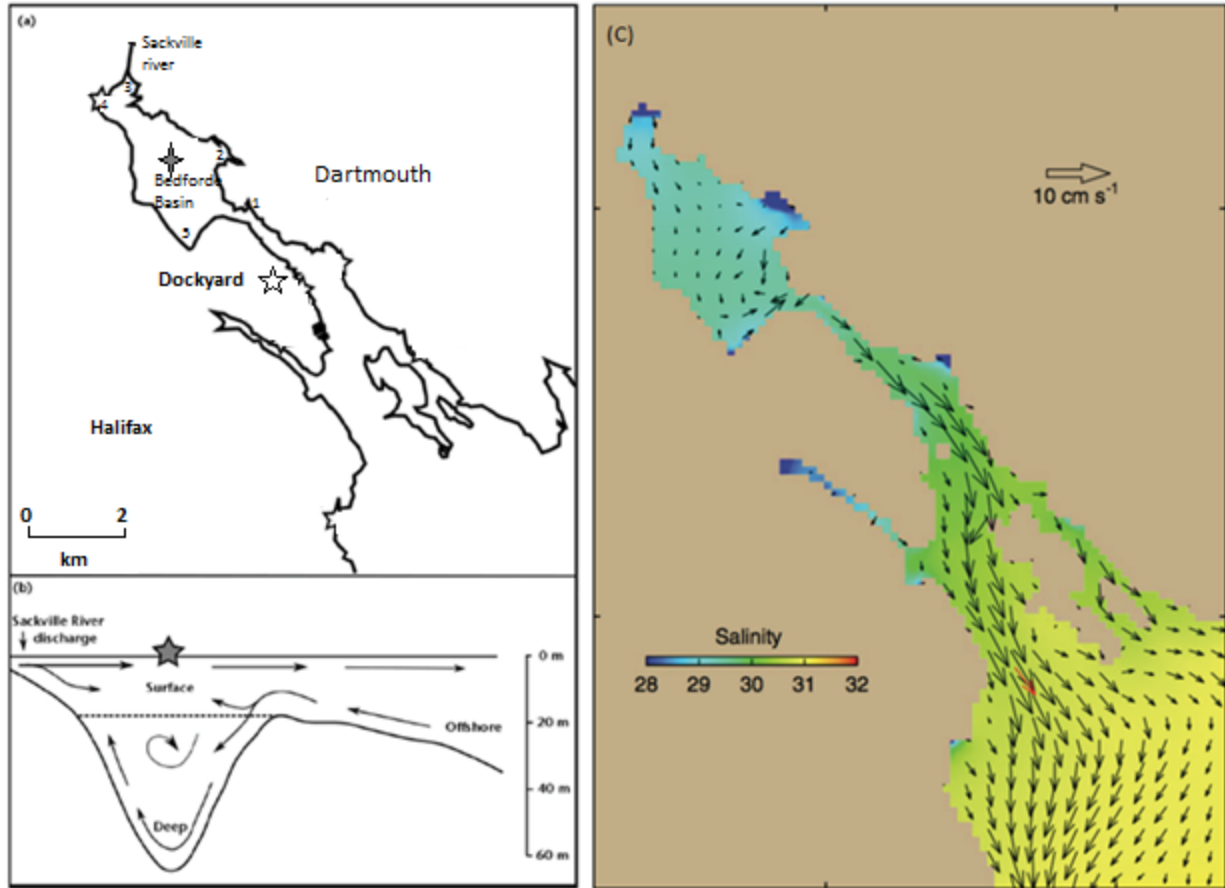
5 Yamamoto, H., Yokouchi, Y., Otsuki, A. and Itoh, H.: Depth profiles of volatile halogenated
6 hydrocarbons in seawater in the Bay of Bengal, Chemosphere, 45(3), 371–377,
7 doi:[http://dx.doi.org/10.1016/S0045-6535\(00\)00541-5](http://dx.doi.org/10.1016/S0045-6535(00)00541-5), 2001.

8 Yokouchi, Y., Osada, K., Wada, M., Hasebe, F., Agama, M., Murakami, R., Mukai, H., Nojiri, Y.,
9 Inuzuka, Y. and Toom-Sauntry, D.: Global distribution and seasonal concentration change
10 of methyl iodide in the atmosphere, Journal of Geophysical Research: Atmospheres,
11 113(D18), D18311, 2008.

12 Yokouchi, Y., Saito, T., Ooki, A. and Mukai, H.: Diurnal and seasonal variations of iodocarbons
13 (CH₂ClI, CH₂I₂, CH₃I, and C₂H₅I) in the marine atmosphere, Journal of Geophysical
14 Research: Atmospheres, 116(D6), D06301, 2011.

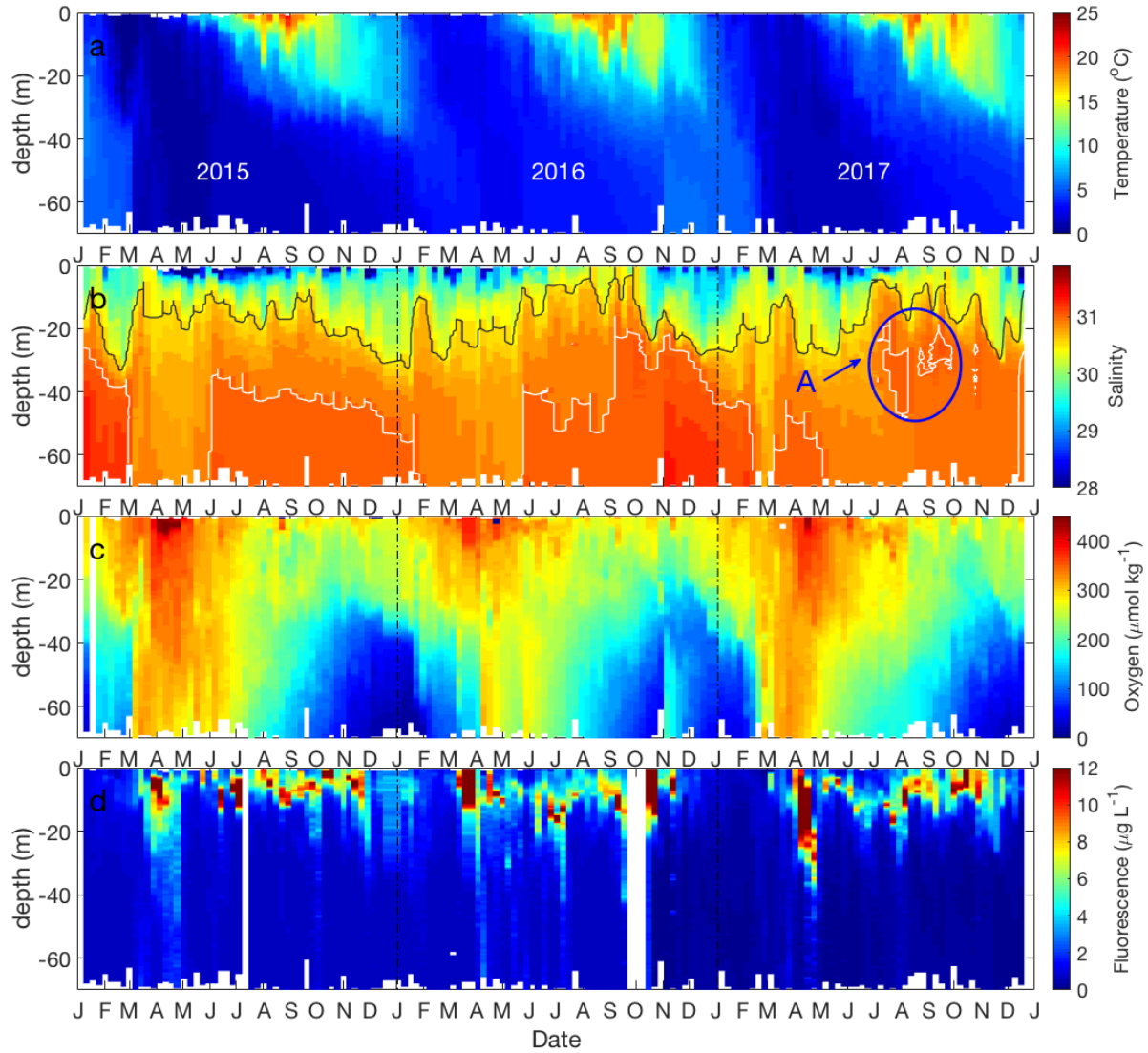
15 Ziska, F., Quack, B., Abrahamsson, K., Archer, S. D., Atlas, E., Bell, T., Butler, J. H., Carpenter, L.
16 J., Jones, C. E. and Harris, N. R. P.: Global sea-to-air flux climatology for bromoform,
17 dibromomethane and methyl iodide, Atmospheric Chemistry and Physics, 13(17), 8915–
18 8934, 2013.

19
20
21
22



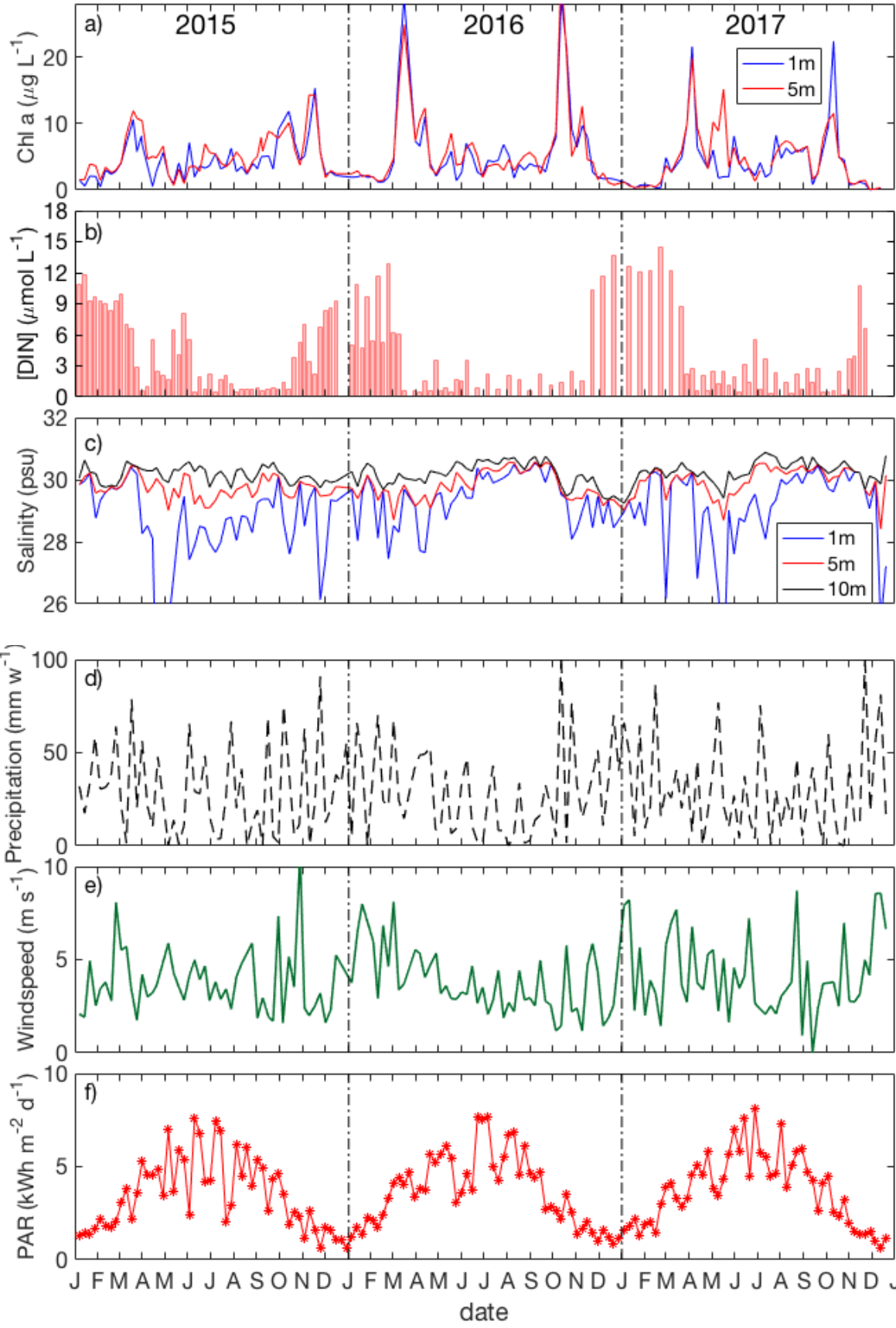
1
2
3
4
5
6

Figure 1. (a): Main sampling location (grey star) and near-shore sampling locations 1-5 (1: Tufts cove; 2: Wrights cove; 3: Sackville; 4: Mill cove; 5: Fairview cove) in Bedford Basin; (b): two layered flow in Halifax Harbour, adapted from Kerrigan et al. (2017); (c): horizontal circulation of water in Halifax Harbour from Shan et al. (2011), using annual mean currents and velocities.

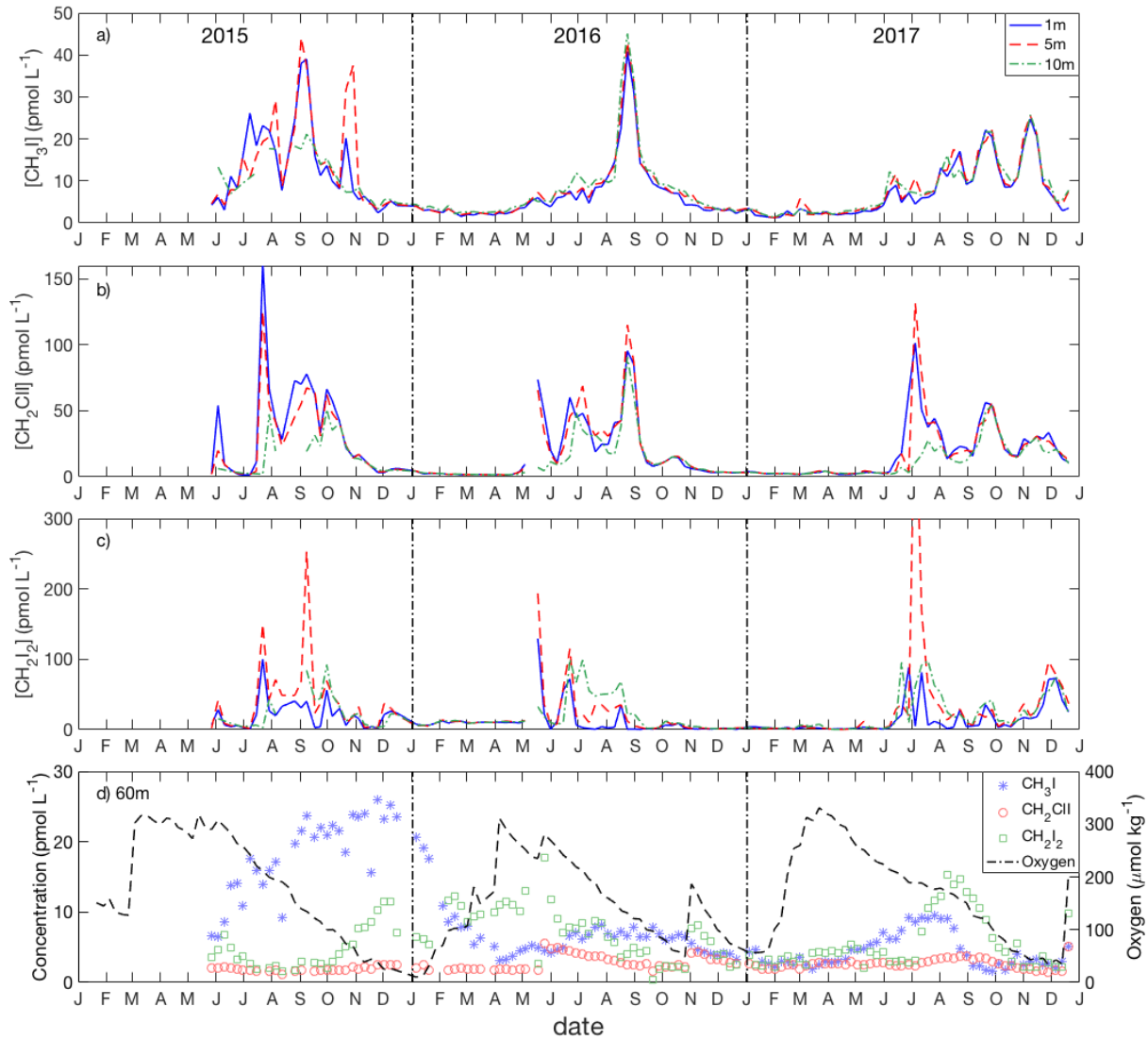


1
2
3
4
5
6
7

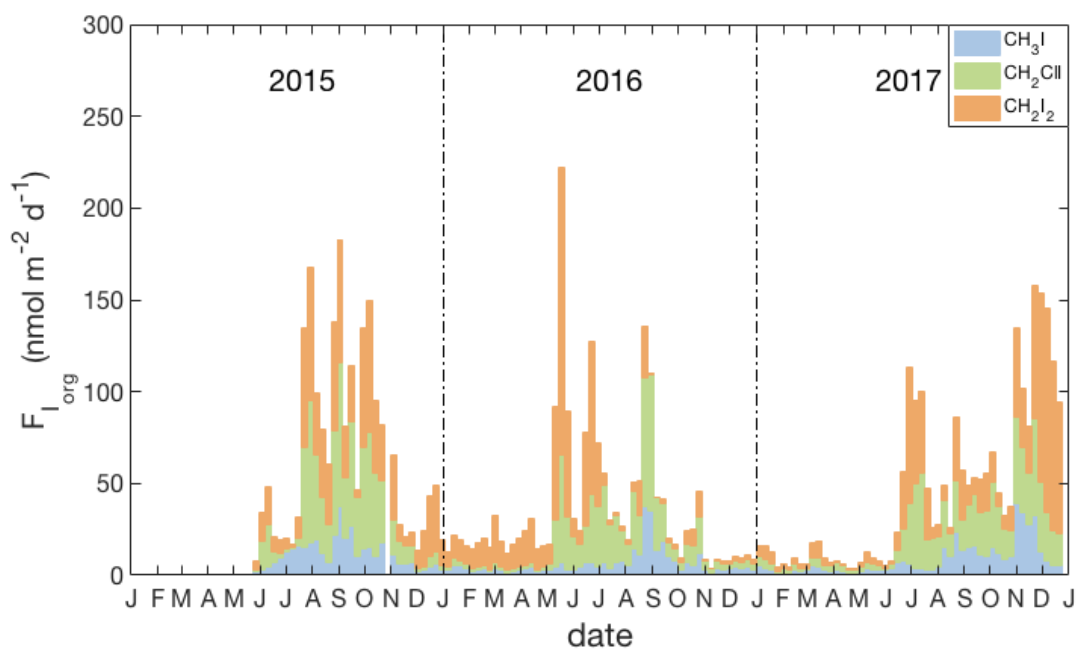
Figure 2. Seasonal patterns of environmental and biological variables in Bedford Basin from January 2015 to Dec 2017. (a) temperature; (b) salinity (grey contour line for $S=30.5$; white contour line for $S=31$). The blue circle (A) highlights a mid-depth intrusion. (c) dissolved oxygen; (d) chlorophyll fluorescence.



1 **Figure 3.** Seasonal variation of (a) chlorophyll α : 1 m (blue line) and 5 m (red line); (b) DIN; (c)
 2 salinity in the surface layer: 1m (blue line), 5m (red line) and 10m (black line); (d) weekly
 3 precipitation and (e) daily averaged windspeed (shown here only for sampling days); (f) weekly
 4 average PAR from January 2015 to December 2017.
 5
 6
 7
 8

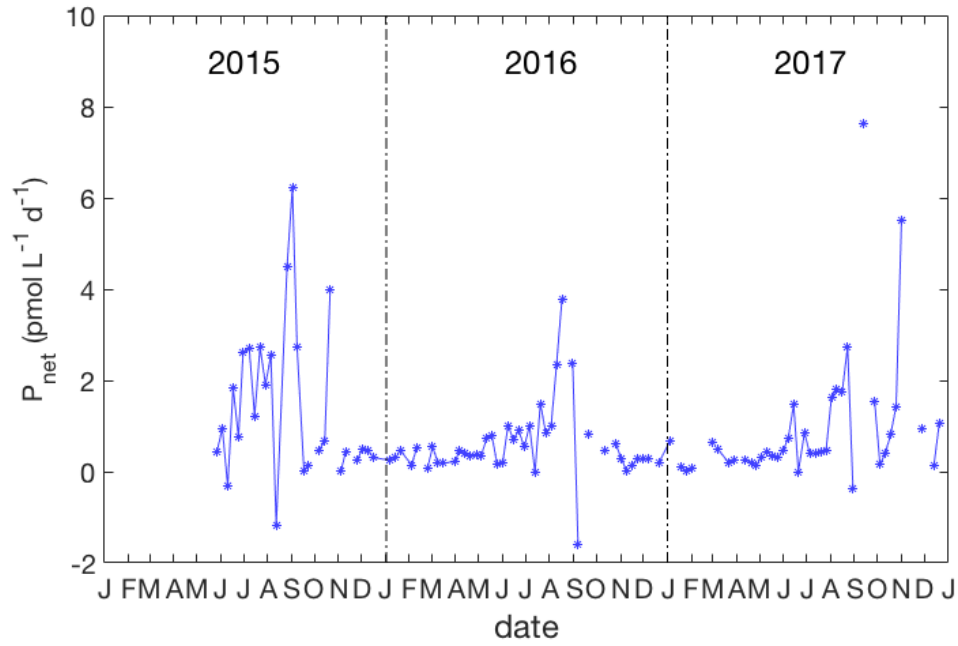


9
 10
 11 **Figure 4.** Seasonal variation of iodocarbons in the Bedford Basin at 1 m (blue line), 5 m (red line)
 12 and 10 m (green line) from May 2015 to December 2017: (a) CH_3I ; (b) CH_2ClI and (c) CH_2I_2 . (d):
 13 time-series from near-bottom water (60m) of iodocarbons and dissolved oxygen.



1
2
3
4
5
6
7
8
9
10
11
12
13
14
15

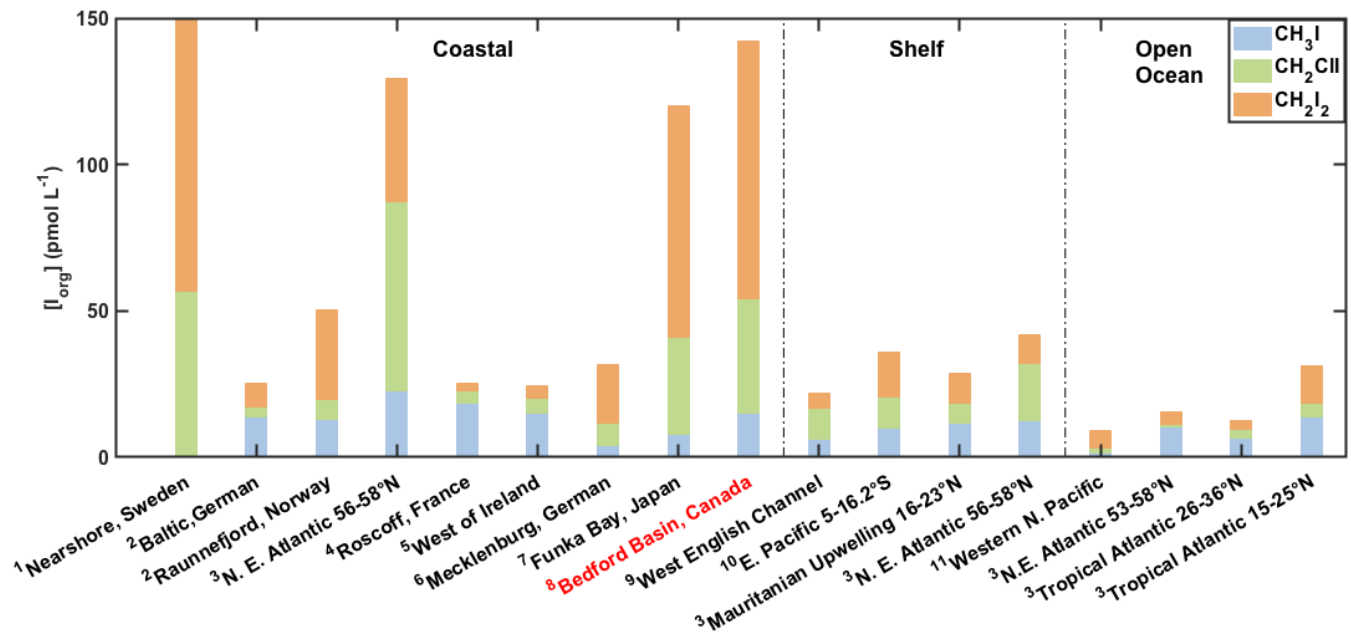
Figure 5 Weekly averages of daily sea-to-air flux estimates of I_{org} (see section 3.3): including relative contributions of individual compounds (blue: CH_3I , green: CH_2ClI and orange: CH_2I_2) and using the parameterization for transfer velocity (k_w) of Nightingale et al. (2000) and for the airside transfer velocity (k_a) of Duce et al. [1991].



1
2
3
4
5
6
7
8
9

Figure 6. Variation of the net production rate of CH₃I in the upper 10 m from 2015 to 2017. No data are plotted when the layer of uniform density extended below 10 m.

1



2

3

4 **Figure 7.** Contribution of Iodocarbons to total organic iodine (I_{org}) in surface seawater from
5 different regions and studies:

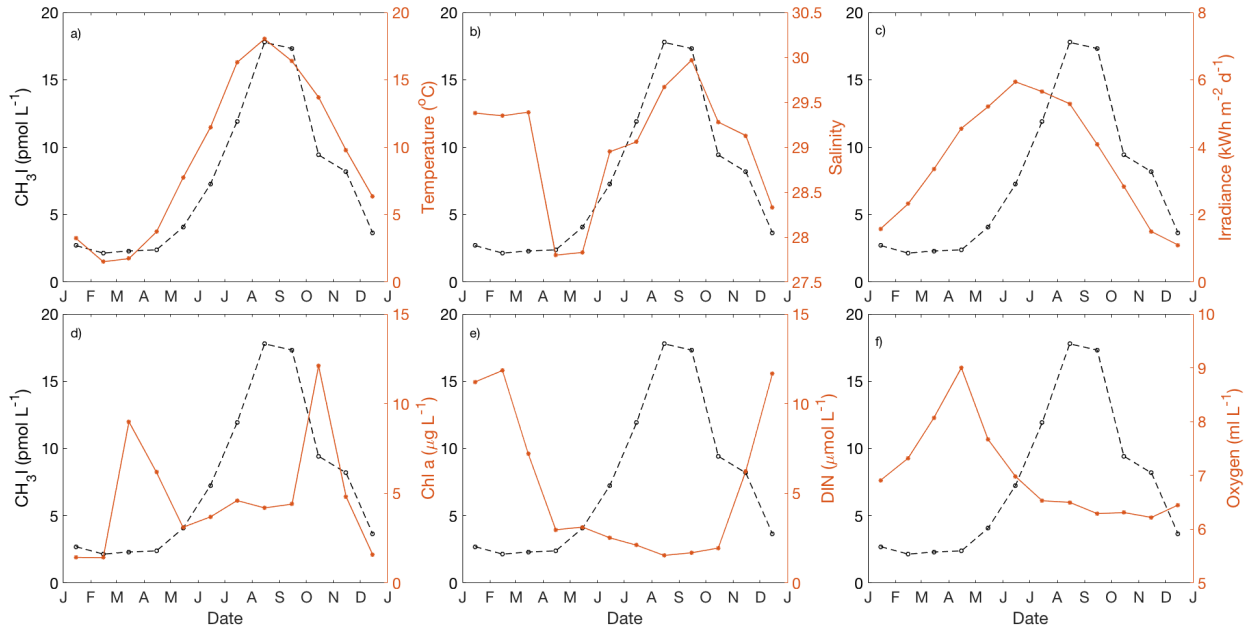
6 1: Klick, 1992; 2: Orlikowski et al., 2015; 3: Jones et al., 2010; 4: Jones et al. 2009; 5: Carpenter
7 et al., 2000; 6: Orlikowski & Schulz-Bull, 2009; 7: Shimizu et al., 2017; 8: this study; 9: Archer et
8 al., 2007; 10: Hepach et al., 2016; 11: Kurihara et al., 2010.

9

10

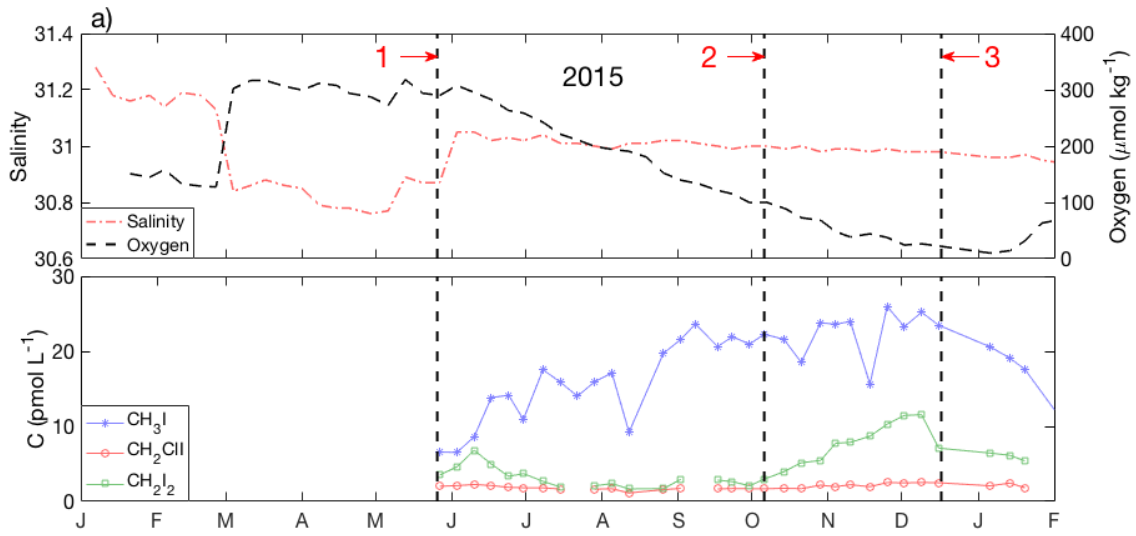
11

12

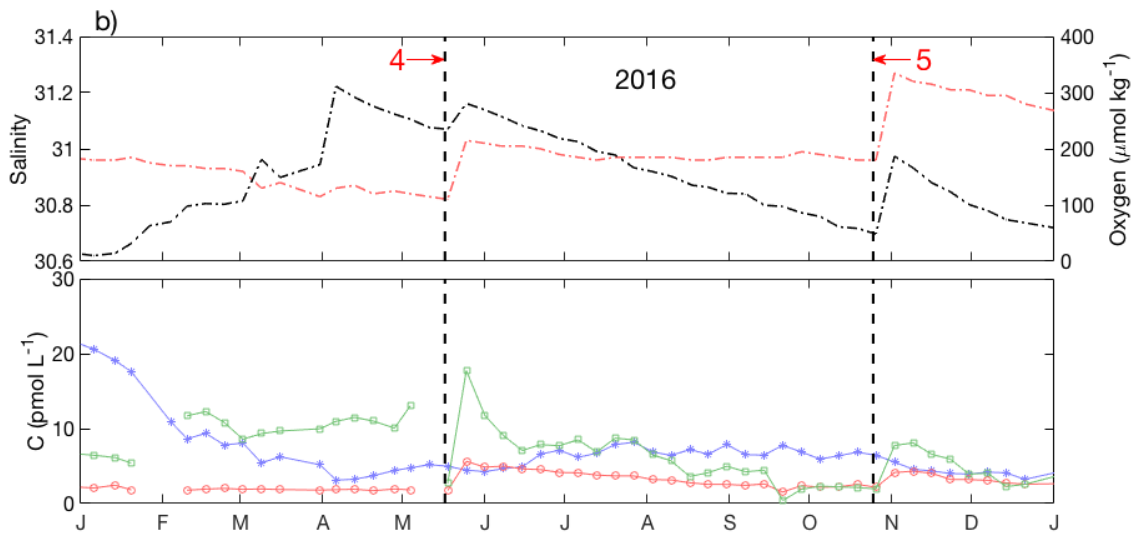


1
 2
 3
 4 **Figure 8.** Annual cycle of (a) temperature, (b) salinity, (c) irradiance, (d) Chl *a*, (e) dissolved
 5 inorganic nitrogen (DIN) and (f) dissolved oxygen for near-surface water (1-5 m) in Bedford Basin.
 6 The black dashed line depicts the annual cycle of CH₃I. The figures present the monthly mean
 7 values based on the data collected from May 2015 to December 2017.

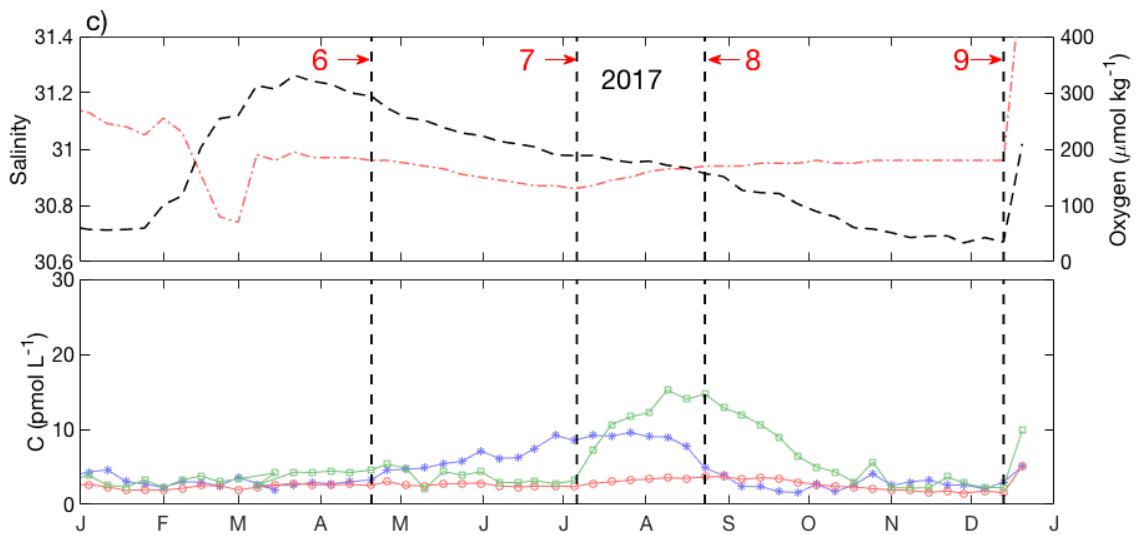
8
 9
 10
 11
 12
 13
 14
 15
 16
 17
 18
 19
 20
 21



1



2



3

1 **Figure 9.** Detailed time-series from near-bottom waters in (a) 2015, (b) 2016 and (c) 2017. For
 2 each year, the upper panel shows variability of salinity (red dash-dot line) and dissolved oxygen
 3 (black dashed line); the lower panel shows iodocarbons (CH_3I : blue stars; CH_2ClI : red open circles
 4 and CH_2I_2 : green open squares). The vertical bold, dashed lines (1 to 9) represent special events
 5 discussed in section 4.5.

6
7

8

9

10

11

12 **Table 1.** R^2 value (Pearson's correlation coefficients, $p < 0.05$) for the individual iodocarbon data
 13 based on both weekly data and monthly average.

	weekly			monthly		
	CH_3I	CH_2ClI	CH_2I_2	CH_3I	CH_2ClI	CH_2I_2
CH_3I (1m)	1.0			1.0		
CH_2ClI (1m)	0.4	1.0		0.7	1.0	
CH_2I_2 (1m)	0.0	0.3	1.0	0.1	0.4	1.0
CH_3I (5m)	1.0			1.0		
CH_2ClI (5m)	0.4	1.0		0.5	1.0	
CH_2I_2 (5m)	0.1	0.4	1.0	0.1	0.6	1.0
CH_3I (10m)	1.0			1.0		
CH_2ClI (10m)	0.7	1.0		0.7	1.0	
CH_2I_2 (10m)	0.1	0.3	1.0	0.2	0.4	1.0

14

15

16

17

1 **Table 2.** R² value (pearson's correlation coefficients, p<0.05) for iodocarbons and potentially
 2 relevant parameters based on both weekly data and monthly average.

	weekly			monthly		
1m	<i>CH₃I</i>	<i>CH₂ClI</i>	<i>CH₂I₂</i>	<i>CH₃I</i>	<i>CH₂ClI</i>	<i>CH₂I₂</i>
SST	0.5	0.4	0.0	0.7	0.6	0.1
SSS	0.1	0.0	0.0	0.1	0.1	0.0
Oxygen	0.3	0.2	0.1	0.3	0.2	0.1
Flu	0.0	0.0	0.0	0.1	0.0	0.0
PAR	0.1	0.1	0.0	0.1	0.3	0.0

3
 4
 5
 6
 7
 8
 9
 10
 11
 12
 13
 14
 15
 16

1 **Table 3.** Seasonal variation of total sea-to-air fluxes of iodocarbons ($\text{nmol m}^{-2} \text{d}^{-1}$). Highest flux
 2 values of iodocarbons in each year are marked in red.

year	season	CH_3I	CH_2ClI	CH_2I_2	I_{org}
2015	Spring				
	Summer	13.9	29.3	15.4	74.0
	Fall	13.1	30.7	13.7	71.2
	Winter	3.6	3.0	8.6	23.7
	Annual	11.9	25.9	14.0	65.9
2016	Spring	3.4	11.8	16.5	48.2
	Summer	12.0	33.2	9.4	64.0
	Fall	7.2	9.4	1.8	20.2
	Winter	3.2	3.0	1.7	9.6
	Annual	6.6	14.4	8.2	37.3
2017	Spring	3.0	2.7	1.7	9.0
	Summer	7.8	22.1	12.1	54.1
	Fall	19.7	31.3	15.9	82.8
	winter	3.2	4.5	9.1	25.9
	Annual	8.5	15.9	10.1	44.7

3
 4
 5
 6
 7
 8
 9
 10
 11
 12

1 **Table 4.** Concentration (pmol L⁻¹) of iodocarbons measured at near shore locations around
2 Bedford Basin as well as at the regular sampling location on July 19, 2017 (1: Tufts cove, 2:
3 Wrights cove, 3: Sackville (rive), 4: Mill cove and 5: Fairview cove) (see Fig. 1a). “Centre” refers
4 to the regular sampling site for the weekly time-series.

5 *Centre Mean for July: the average (and std. deviation) of measurements at the regular, weekly
6 sampling location during the month of July 2017 (n=4).

7

	CH ₃ I	CH ₂ ClI	CH ₂ I ₂
¹ Tufts cove	5.8	35.5	8.8
² Wright's cove	6.7	20.6	12.5
³ Sackville	3.8	6.5	4.9
⁴ Mill cove	8.3	28.0	18.6
⁵ Fairview cove	6.2	26.3	6.4
Middle of Bedford Basin	6.1	37.6	6.3
*Centre Mean for July	5.9±0.9	58.5±25.2	26.1±32.0

8

9

10

11

12

13

14

15

16

17

18

1 **Table 5.** Comparison of sea-to-air flux ($\text{nmol m}^{-2} \text{d}^{-1}$) of total organic iodine from different studies.
 2 English Channel is an average for 1 year; Funka Bay value is average over 3 years; Kiel Fjord is
 3 average over 2 years but for CH_3I only; Bedford Basin (this study) is an average over 3 years.
 4 Seasons as defined in this study (see section 2). For Funka Bay, values in parentheses represent
 5 fluxes that have been adjusted from the original reported values to take into account effect of air-
 6 side resistance, using correction factors of 12 and 28 % for CH_2ClI and CH_2I_2 respectively (based
 7 on average effects reported in Archer et al. (2007) and this study; see section 4.6).

8

	English Channel		Funka Bay		Kiel Fjord		Bedford Basin	
	Archer et al.(2007)		Shimizu et al. (2017)		Shi et al. (2014)		This Study	
Season	Total	%- CH_3I	Total	%- CH_3I	Total	%- CH_3I	Total	%- CH_3I
Spring			15.3(12.8)	33.8(40.3)	2.8		28.6	11.1
Summer			113.3(86.6)	4.7(6.2)	5.2		64.0	17.5
Fall			47.6(41.1)	32.5(37.6)	2.2		58.1	23.0
Winter			27.5(22.5)	22.3(27.2)	0.2		19.7	16.8
Annual	42.6	27.9	54.8(43.5)	14.0(17.6)	3.3		46.7	19.3

9